| OF |
AD
A034489

END

DATE
FILMED

2-7

ADA034489

ISOLATION AND ABSORPTION OF MACHINERY VIBRATION, A LECTURE
GIVEN AT THE ARL/NAVSEA "WORKSHOP ON THE REDUCTION OF
NOISE AND STRUCTURAL VIBRATION," APRIL 26, 1976

J. C. Snowdon

Technical Memorandum
File No. TM 76-188
July 1, 1976
Contract No. N00017-73-C-1418

Copy No. 57

D D C
RECEIVED
JAN 18 1977
A

The Pennsylvania State University
Institute for Science and Engineering
APPLIED RESEARCH LABORATORY
P. O. Box 30
State College, PA 16801

NAVY DEPARTMENT

NAVAL SEA SYSTEMS COMMAND

REPORT DOCUMENTATION PAGE		READ INSTRUCTIONS BEFORE COMPLETING FORM
1. REPORT NUMBER ⑭ TM-76-188 ✓	2. GOVT ACCESSION NO.	3. RECIPIENT'S CATALOG NUMBER
4. TITLE *(and Subtitle)* ⑥ ISOLATION AND ABSORPTION OF MACHINERY VIBRATION ⑨		5. TYPE OF REPORT & PERIOD COVERED *Technical memo.*
		6. PERFORMING ORG. REPORT NUMBER
7. AUTHOR(s) ⑩ J. C. Snowdon ⑯ F43452 ⑰ SF 43452702		8. CONTRACT OR GRANT NUMBER(s) ⑮ N00017-73-C-1418 ✓
9. PERFORMING ORGANIZATION NAME AND ADDRESS The Pennsylvania State University ✓ Applied Research Laboratory P. O. Box 30, State College, PA 16801		10. PROGRAM ELEMENT, PROJECT, TASK AREA & WORK UNIT NUMBERS SF 43-452-702 (Nav Sea) N00014-76-RQ-00002(ONR)
11. CONTROLLING OFFICE NAME AND ADDRESS Naval Sea Systems Command Office of Naval Research Department of the Navy Department of the Navy Washington, DC 20362 Arlington, VA 22217		12. REPORT DATE July 1, 1976
		13. NUMBER OF PAGES 60
14. MONITORING AGENCY NAME & ADDRESS*(If different from Controlling Office)* ⑪ 1 Jul 76 ⑫ 54 p.		15. SECURITY CLASS. *(of this report)* UNCLASSIFIED
		15a. DECLASSIFICATION/DOWNGRADING SCHEDULE

16. DISTRIBUTION STATEMENT *(of this Report)*

Approved for public release; distribution unlimited. Per NAVSEA
Nov. 22, 1976

17. DISTRIBUTION STATEMENT *(of the abstract entered in Block 20, if different from Report)*

18. SUPPLEMENTARY NOTES

19. KEY WORDS *(Continue on reverse side if necessary and identify by block number)*

Vibration isolation.   Dynamic vibration absorbers.
Antivibration mountings.   Nonrigid substructures.
Machinery vibration.

20. ABSTRACT *(Continue on reverse side if necessary and identify by block number)*

The isolation of machinery vibration from rigid and nonrigid substructures is described in uncomplicated terms. One- and two-stage mounting systems, single and multiple antivibration mountings, and beamlike and platelike substructures are examined. A machine and the intermediate mass of a two-stage mounting system are considered to be supported by flanges or feet to demonstrate the loss in isolation that can occur if the flanges are not rigid but are multiresonant because of their poor design. The use of conventional dynamic absorbers to reduce the vibration of such

(cont. on p1475B)

(cont to p 1473A)

↳ structural members as beams (rails and stanchions) and circular plates
(bulkheads) is discussed. A novel dynamic vibration absorber is described
that comprises a damped circular plate loaded centrally by a lumped mass
and clamped at its perimeter to the vibrating item or structure of concern.

ABSTRACT

The isolation of machinery vibration from rigid and nonrigid substructures is described in uncomplicated terms. One- and two-stage mounting systems, single and multiple antivibration mountings, and beamlike and platelike substructures are examined. A machine and the intermediate mass of a two-stage mounting system are considered to be supported by flanges or feet to demonstrate the loss in isolation that can occur if the flanges are not rigid but are multiresonant because of their poor design. The use of conventional dynamic absorbers to reduce the vibration of such structural members as beams (rails and stanchions) and circular plates (bulkheads) is discussed. A novel dynamic vibration absorber is described that comprises a damped circular plate loaded centrally by a lumped mass and clamped at its perimeter to the vibrating item or structure of concern.

PRINCIPLES OF VIBRATION ISOLATION

Figure 1(a) shows a machine of mass M supported by an antivibration mounting on an ideally rigid foundation such as a concrete factory floor. This is the simplest idealization possible. To the foundation is transmitted a force $\tilde{F}_2$ that is produced by a sinusoidally varying force $\tilde{F}_1$ applied to or generated within M. The mount is visualized as a rubber spring with a stiffness K and with internal damping described by a damping factor δ_K = 0.05, a value that typifies, for example, the damping of natural, neoprene, and SBR rubbers. The values of K and δ_K are assumed to be frequency independent.

A quantity of basic interest for this so-called simple mounting system is transmissibility T, which is defined as the magnitude of the force ratio $|\tilde{F}_2/\tilde{F}_1|$. This ratio is shown on a decibel scale as a function of a frequency ratio $\Omega = \omega/\omega_0$ in Figure 2. Here, $20 \log_{10} T$ is plotted versus the ratio Ω of the exciting angular frequency ω to the natural angular frequency $\omega_0 = \sqrt{(K/M)}$ of the mounting system. Negative values of TdB mean that the input force has been attenuated; positive values of TdB mean that undesired magnification has occurred at and near the system resonance. Only for values of $\omega > \sqrt{2}\,\omega_0$ does the mount provide the desired attenuation of transmitted force shown by the hatched area. Consequently, to assign to ω_0 the smallest value possible without endangering the lateral stability of the mounting system should always be an advantage. The level of the transmitted vibration may appear to be very low at high frequencies, but it must be recognized that even small amounts of vibratory energy can excite the resonant modes of neighboring (and sometimes of distant) platelike structures, and that many of the plate modes will be relatively efficient radiators of unwanted noise.

Now, larger values of transmissibility (that is to say, reduced isolation) may occur at frequencies above resonance than Figure 2 predicts. The reasons may simply be mechanical or they may be basic:

(1)   In the first case, isolation may be impaired by mechanical links that have significant stiffness and hence that bypass, to some extent, the antivibration mount. Vibration from a resiliently mounted diesel engine, for example, may reach its foundation via an exhaust pipe that is still rigidly connected to a surrounding enclosure. Or vibration may reach the foundation via a bearing pedestal that supports a rotating shaft extending from the engine.

(2)   In the second case, transmissibility may be greater than predicted at high frequencies because the mounting system considered here is then too simplified a model of the practical situation; for example, the antivibration mount may cease to behave as an ideally resilient member at high frequencies. In this event, so-called wave effects will occur at frequencies for which the mount dimensions become comparable with multiples of the half wavelengths of the elastic waves traveling through the mounting. At these frequencies, resonant peaks appear in the transmissibility curve. However, these peaks will not always be of primary concern for two reasons: (a) even the first of the peaks will invariably occur at frequencies higher than $20 \omega_o$, where significant isolation already exists, and (b) the peaks will be suppressed to some extent by the internal damping of the rubber mount.

One further reason why the high-frequency isolation may be impaired is of sufficient interest to be discussed now in some detail. Thus, in some cases, as in Figure 1(b), the machine will be supported via flanges or feet that may not be ideally rigid but may be multiresonant, so giving rise to other peaks in the transmissibility curve at high frequencies. These peaks may well be troublesome because the internal damping of the metal feet will be at least 10 times smaller than the damping of the rubber mounts beneath them. The feet may protrude from the bottom of the machine, or from its sides as shown. This will be the case if the beneficial step is taken to place the feet in a plane that passes through the center of gravity of the machine (so minimizing the rocking motion it experiences when subjected to horizontally directed forces). A guide to the force transmissibility T across this simple system has been obtained by idealizing the machine feet as short shear beams; that is, as beams with *length-to-depth* ratios of approximately 3 or less for which it can realistically be assumed that the beam deflection due to bending is much less than the deflection due to shear.

Representative calculations of T are plotted in Figure 3 for machine feet having 1/40 of the machine mass, a damping factor $\delta_f = 0.01$, and stiffnesses 5, 25, and 100 times greater than the stiffness of the mounts that support them from below. The resonances of the machine feet, which are responsible for the pronounced peak values of T at high frequencies, are seen to be of the least consequence when the stiffness ratio is largest. In fact, the resonances will advantageously occur at the highest possible frequency when the ratio of the static stiffness to mass of the feet is made as large as possible; that is, in this simple example, when the shear-beam feet are made as short as possible.

This is not a contrived problem; in fact, one does not have to look

far to find examples of exactly this situation, as Figures 4 and 5 show. In Figure 4, a marine engine is attached to a subframe fashioned so that the mounting points lie on the same horizontal as the center of gravity of the engine. In Figure 5, an axial flow fan with vertical discharge is mounted resiliently on a subframe with members having significant unsupported lengths.

COMPOUND MOUNTING SYSTEM

It is natural to question how it is possible to obtain greater vibration isolation than that afforded by the simple mounting system. Well, if added mass can be tolerated, the two-stage or compound mounting shown in Figure 6(a) can provide especially low values of transmissibility at high frequencies. Antivibration mounts in the upper and lower stages of the system are separated by an additional or intermediate mass M_2. The system possesses a secondary as well as a primary resonance, which is a disadvantage, but above the secondary resonance, transmissibility falls off as $1/\omega^4$ (that is, at 24 dB/octave). This is twice the rate of 12 dB/octave at which the transmissibility of the simple system decreases at high frequencies.

Figure 7 shows the calculated force transmissibility across three compound systems with natural rubber mounts and with intermediate masses 10, 20, and 100% as large as the machine mass. The dashed-line curve shows the transmissibility across the simple system. The potential value of the compound system as an especially effective antivibration mounting at high frequencies is immediately apparent. The system can be of particular value in mitigating the increase in transmissibility that occurs, for example, when it is necessary to mount machinery on a non-rigid foundation such as a system of steel girders in shipboard applications. The foundation reso-

nances are then superimposed, approximately speaking, on one of the lower solid-line curves rather than on the dashed-line curve.

A small-scale application of the compound system is shown in Figure 8 (after E. G. Fischer and H. M. Forkois). Here the motor-driven compressor of a refrigerator is isolated from its housing by steel springs carrying intermediate masses. Additional mass has also been used to block vibration transmission along the refrigerant line.

Figure 9 shows the compound mounting of 17,000 lb and 80,000 lb diesel generators on one extensive intermediate mass in a Canadian oceanographic vessel (after R. M. Gorman). It is always advantageous to employ the largest possible intermediate mass M_2 because, at high frequencies, transmissibility is essentially proportional to $1/M_2\omega^4$. But if the compound system is to provide the small values of transmissibility as predicted, it is vital that M_2 remains masslike at high frequencies. If it does not, then the performance of the system will be seriously impaired.

This situation is shown in Figure 6(b), where the flanges from which M_2 is supported behave as springs at some high frequencies because of their poor design. If we again model these multiresonant flanges as short shear beams, the transmissibility across the system can be calculated and plotted as in Figure 10. Here, the intermediate mass M_2 has one-fifth of the machine mass. The dashed-line curve shows the transmissibility across the simple system. The solid-line curve shows the transmissibility across the compound system when M_2 is ideally rigid and masslike and the system is totally effective at high frequencies. The chain-line curve shows how transmissibility changes when the multiresonant flanges are 1/40 as massive as M_2 and 5 times stiffer than the mounts of the compound system that support them from below; their internal damping factor $\delta_f = 0.01$. Pronounced peaks

now appear in the transmissibility curve at high frequencies where the shear-beam flanges resonate, their ends having large motion and their roots, which are attached to the mass M_2, having relatively small motion. In addition, pronounced minima occur in the transmissibility curve at frequencies for which the flange ends have little motion and their roots, together with M_2, have relatively large motion. In fact, M_2 and the flanges actually behave in the manner of a dynamic vibration absorber at these frequencies. Thus, it is vital that the intermediate mass always be designed to remain masslike and rigid to the highest possible frequency.

NONRIGID FOUNDATIONS

Let us turn now to the problem of isolating machinery vibration from nonrigid foundations; that is, foundations that have many self resonances. This problem is of permanent concern in marine and aeronautical applications. It is becoming of greater concern in land-based applications where increased mention is being made, for example, of steel-frame rather than massive concrete foundations for large modern turbines and auxilliary equipment.

One nonrigid foundation and mounting system is shown in Figure 11(a). The foundation comprises an internally damped clamped-clamped beam of half-length a, mass M_b, and small internal damping factor $\delta_E = 0.01$. The transmissibility across this system, which is defined as the magnitude of the total output force $2\tilde{F}_2$ divided by the impressed force $\tilde{F}_1$, is plotted in Figure 12 as the solid-line curve for which the machine is 10 times more massive than the nonrigid foundation beam beneath. As before, the horizontal axis is the ratio of the impressed frequency to the natural frequency ω_0 of the mounting system calculated as though the foundation were ideally rigid. The fundamental resonance of the foundation is always assumed to occur at

a frequency of $10\omega_o$ so that, if $\omega_o/2\pi$ = 5 Hz, the first foundation resonance would occur at 50 Hz. The peaks in the solid-line transmissibility curve where $\Omega \geq 10$ correspond to the first, second, third, and fourth symmetrical resonances of the foundation beam. The peaks represent an unfortunate loss in isolation as compared with the transmissibility of the simple mounting system, which is shown by the dashed-line curve.

A more complex calculation of transmissibility can be made, for example, for the mounting system of Figure 13, where not one but eight antivibration mounts support the mass M. The mounts, each of stiffness K = K/8 in the former notation, are spaced as shown at equal intervals along the beam. The chain-line curve of Figure 12 shows that, for this mount configuration, which represents closely the performance of a rail-type mount of continuous run, beneficially smaller peak values of transmissibility result at high frequencies. In addition, troughs appear in the chain-line curve at frequencies for which the forces exerted on the beam by the multiple antivibration mountings produce forces of different phase at the beam terminations that conflict with one another to produce minima in the net transmitted force.

Let us continue now to a problem of intermediate complexity as shown in Figure 14, where two mounts support the machine. The mounts lie equidistant from the beam center but their location is otherwise arbitrary. One can also attach a dynamic vibration absorber of small mass M_a to the center of the beam, as in Figure 14(b), or to the beam at each mount location; or divide the beam into two spans by a central inflexible prop or clamp, as in Figure 14(c); or load the beam by additional lumped masses M_a placed beneath each antivibration mount, as in Figure 14(d). In Figure 14(b), the dynamic absorber is tuned to suppress the fundamental resonance of the foundation beam (which is potentially the most troublesome resonance). At or near this

resonant frequency the motion of M_a is large -- whereas the motion of the foundation beam and the force transmissibility to its terminations are minimized.

Representative calculations of the transmissibility across the systems of Figures 14(a), (b), and (c) -- that is, the total output force divided by the impressed force $\tilde{F}_1$ in each case -- are compared in Figure 15 for a machine that is again ten times more massive than the nonrigid foundation beam beneath it, and for an attached dynamic absorber that is one-fourth as massive as the beam. The antivibration mounts are located at a distance of one-quarter of the beam length from each termination.

Shown in Figure 15 by the dashed-line curve is the transmissibility across the basic system of Figure 14(a). The transmissibility peak at the first beam resonance, which is again assigned the frequency $10\omega_o$, is the most pronounced and potentially the most troublesome of the higher-frequency peaks, which again occur at the first, second, third, and fourth symmetrical resonances of the foundation beam. The solid-line curve shows how the magnitude of the first of the higher-frequency peaks can be reduced effectively if a dynamic absorber of optimum design is attached to the center of the foundation beam. In fact, the dynamic absorber is surprisingly efficient in reducing transmissibility in view of its relatively small mass; moreover, not only is it effective in suppressing the resonance to which it is tuned, but its moderately large damping is also effective in suppressing the resonances at higher frequencies.

Finally, the chain-line curve of Figure 15 shows how transmissibility changes when the dynamic absorber is removed from the center of the foundation beam and is replaced there by a rigid support or clamp where the beam displacement and slope are constrained to zero. The original beam of length

2a is thus divided into two spans of length a; these spans possess first, second, third, etc., resonant frequencies that are essentially 2^2 or 4 times higher than those of the original beam. Consequently, even though the "abruptness" of the higher-frequency peaks is essentially unchanged, their levels are significantly reduced because of the increased effectiveness of the antivibration mounts at these frequencies; in fact, the first two of the higher-frequency peaks have fallen in level by approximately 15 and 23 dB, which is a factor of 14 in magnitude.

MULTISPAN BEAMS

Just as it has proven to be an advantage to halve the length of the foundation beam, it also proves to be an advantage to repeat the procedure, so that the beam is provided with a four-span support. This situation is shown by the partial view of Figure 16, where four antivibration mounts, one at the center of each span of length a/2, together isolate the machinery vibration via multiresonant flanges or feet that extend from the side of the machine in the plane of its center of gravity. Calculations of the force transmissibility across this system (the magnitude of $|8\tilde{F}_2/\tilde{F}_1|$) are plotted in Figure 17 for shear-beam feet that together have 1/40 of the machine mass, a small internal damping factor $\delta_f = 0.01$, and 5 times greater stiffness than the mounts beneath them. The machine is again 10 times more massive than the foundation beam. The fundamental resonant frequency of the foundation -- originally observed where $\Omega = \omega/\omega_0 = 10$, and then where $\Omega = 40$ for the foundation beam of dual span, has now been increased again, through division of the beam into four spans, by a further factor of 4 to appear here where $\Omega = 160$. The companion transmissibility peak at this high frequency (800 Hz if $\omega_0/2\pi = 5$ Hz) is now of less consequence than the peaks observed at

the first two resonances of the machine feet that occur at lower frequencies. This only serves to emphasize the need to design the machine feet with considerable care to ensure that their resonances always fall at the highest possible frequency.

Note that the mounts have always been placed symmetrically about the midpoints of the original foundation beam, or they have been located at midspan on the multispan beams considered. In this way, only the symmetrical beam modes have been excited. For other locations of the mounts, both the symmetrical and the antisymmetrical modes would be excited so that the number of transmissibility peaks in the preceding figures would be detrimentally increased; in fact, it would essentially be doubled.

PLATELIKE FOUNDATIONS

Mention must also be made of the companion problem of mounting machinery on platelike foundations -- that arises, for example, in machinery rooms aboard surface ships and in machinery rooms located on the top levels of high-rise buildings. This problem is modeled in Figure 11(b), where an item of machinery is centrally mounted on an internally damped, simply supported square plate. Here, the transmitted force $\tilde{F}_2$ comprises four concentrated forces, one at each plate corner, plus a distributed force shown by the dotted regions along the plate boundaries.

One calculation of the force transmissibility $T = |\tilde{F}_2/\tilde{F}_1|$ across the mounting system is plotted as the solid-line curve in Figure 18. The machine has 4 times the mass of the platelike foundation, which is assumed to have a fundamental resonant frequency of $4\omega_o$, where ω_o is again the natural frequency of the mounting system calculated as though the foundation were ideally rigid. The internal damping factor of the plate $\delta_F = 0.01$.

Note that the first transmissibility peak occurs at a smaller value of the frequency ratio $\Omega = \omega/\omega_0$ than 1.0 because the effective mount stiffness is reduced by the plate flexibility. Again, the second transmissibility peak (corresponding to the first foundation resonance) occurs at a greater value of Ω than 4 because the natural frequencies of the platelike foundation are shifted to higher frequencies by the springlike constraint of the central antivibration mount. The transmissibility curve detrimentally shows a great many resonant peaks at high frequencies. More peaks would possibly be evident if the platelike foundation were moderately rectangular rather than square, because the foundation would then have fewer degenerate modes (those having overlapping natural frequencies). Either way, there is increased likelihood of the disturbing frequencies coinciding with one or more natural frequencies of the foundation.

For comparison, the chain-line curve shows how transmissibility changes when the square foundation is replaced by an internally damped circular plate with a simply supported boundary. The mass and frequency ratios are equal to 4, as before. The density of the foundation resonances is now less than one-half that observed previously, which suggests that it may be beneficial to investigate further the possibility of mounting machinery on circular rather than square platelike floor areas. Such an area, for example, could be supported around its perimeter by a rigid circular rib and be separated by an expansion joint from the adjacent floor areas of the square machinery room in which it is located.

Figure 19 shows other basic situations that have recently been analyzed; in (a), an item of machinery is supported by four symmetrically located antivibration mounts on the floor of a rectangular machinery room. In (b), dynamic vibration absorbers are attached to the floor at points immediately

beneath the mounts, thus providing a remedy for bad situations in existing structures. In (c), the floor area in a proposed structure is divided by expansion joints into four like quadrants, each of which is driven by the force transmitted by a single mount only, and which is vibrating independently of the three other quadrants. Because the quadrants have a fundamental resonant frequency 4 times higher than that of the original floor, the vibration levels and transmitted forces at the new fundamental resonance, and at higher resonances, are significantly reduced because of the greater effectiveness of the antivibration mounts at these higher frequencies.

DYNAMIC VIBRATION ABSORBERS

Dynamic vibration absorbers have been mentioned in our prior discussions. Let us now consider their application in other circumstances, and initially examine an absorber attached to a simple mass-spring vibrator, as in Figure 20.

The absorber comprises a mass M_2 that is attached via a single spring and damper to a vibrating item of mass M_1, the displacement $\tilde{x}_2$ of which is found to be excessive under the action of a vibratory ground displacement $\tilde{x}_1$ or, equivalently, a sinusoidally varying force applied to M_1. In either case, the vibrating item M_1 is considered to resonate on resilient members of total stiffness K_1. The mass M_2 is tuned to resonate at a similar frequency at which its motion becomes relatively large, whereas the motion of M_1 is minimized. For an instrument mounting, M_2/M_1 might be as large as 1.0; whereas, for a vibrating item of machinery, M_2/M_1 would be unlikely to exceed 0.2, for example. Initially, consider that the primary system has negligible damping.

Figure 21 shows the transmissibility $T = |\tilde{x}_2/\tilde{x}_1|$ across the system when the dynamic absorber is also undamped. Transmissibility takes a minimum value at the angular frequency ω_a to which the absorber is tuned. "Compensating" peaks are introduced on each side of this minimum. The compensating peaks can be effectively suppressed by damping the absorber, but the depth of the trough is then detrimentally reduced.

The transmissibility obtained when the absorber is infinitely damped (rigid connection between M_1 and M_2) is shown by the second curve that intersects the former curve at so-called fixed points A and B for which transmissibility is equal to T_a and T_b, respectively. The transmissibility curves for all other values of absorber damping intermediate to zero and infinity likewise pass through the points A and B.

Classically, the absorber is said to be optimumly tuned if its natural frequency is such that the fixed points A and B lie on the same horizontal, at which time $T_a = T_b$. Optimum absorber damping is said to be that for which the compensating peak just to the left of point A is equal in height to T_a, and the compensating peak just to the right of point B is equal in height to T_b. Hence, because $T_a = T_b$, the two damped peaks take equal values. These conditions of tuning and damping are said to be optimum because, if the absorber is differently tuned and damped, either the left-hand peak is higher than the right-hand peak, or vice versa. In any case, the higher of the two peaks always exceeds the common level that the peaks share for conditions of optimum absorber tuning and damping.

Figure 22 shows the transmissibility calculated for an optimumly tuned absorber that is 1/5 as massive as the mounted item; the absorber damping is assumed to be viscous and, in turn, to be equal to 10, 20, 40, and 100 percent of critical. Note that the fixed points lie on the same horizontal

as well as can be drawn. Also note that damping of 10 or 20 percent of critical is inadequate because the peak heights remain unequal. Damping of 40 or 100 percent of critical is too large because the two peaks have coalesced to form single peaks of large amplitude. Optimum damping is actually 25 percent of critical, and calculations made for this case, and for three other optimum cases are plotted in Figure 23.

The mass ratio μ referred to in Figure 23 is defined as follows:

$$\mu = M_1 / (M_1 + M_2) \ .$$

Thus, values of $\mu = 50/51$, $10/11$, $5/6$, and $1/2$ relate to absorbers that are $1/50$, $1/10$, $1/5$, and equally as massive as the mounted item. Transmissibility is plotted versus the ratio Ω of the angular frequency of excitation ω to a reference frequency ω_o, which is now the natural frequency of the one-degree-of-freedom system obtained when the absorber mass M_2 is connected rigidly to M_1. Optimum values of the absorber tuning and damping ratios $(n)_{opt}$ and $(\delta_R)_{opt}$ are given by the simple equations

$$(n)_{opt} = (\omega_a/\omega_o)_{opt} = \sqrt{\mu}$$

and

$$(\delta_R)_{opt} = \sqrt{[3(1 - \mu)/8]} \ .$$

The advantage of introducing relatively large masses to reduce transmissibility is clearly apparent in Figure 23. In all cases, transmissibility is suppressed effectively and symmetrically at resonance, yet transmissibility at high frequencies decreases at 12 dB/octave.

Examples of small- and large-scale applications of the dynamic absorber are shown in Figures 24 and 25. In Figure 24, a ring of high-damping rubber-

like material provides both the stiffness and the damping for a lightweight
absorber tuned to suppress the fundamental resonance of a beam or panel
(after D. I. G. Jones, A. D. Nashif, and R. L. Adkins). In Figure 25, a
dynamic absorber is tuned to reduce the vibration in the vicinity of a pilot's
seat (above point 1) in a helicopter (after J. J. Sciarra). To reduce other
than local vibration of the helicopter, the use of additional absorbers at
other locations would be necessary.

The question remains -- is it not possible to improve the performance of
the dynamic absorber; namely, is it not possible to suppress the compensating
peaks and yet retain the significant trough introduced by the absorber in
the transmissibility curve? This, in fact, does prove to be feasible if it
is possible to damp the primary system of Figure 20 heavily (with half-
critical viscous damping, for example) and to employ a dynamic absorber with
only a small damping factor ($\delta = 0.01$, for example). The compensating peaks
can then be avoided and a trough of significant magnitude generated, as
illustrated in Figure 26. Here are shown transmissibility curves for an
absorber tuned successively to three different frequencies (ω_a/ω_o = 0.667, 1.0,
and 1.5); the absorber mass ratio $\mu = 5/6$. It is apparent from these results
that a sharp minimum, indicating desired attenuation, can be introduced at
essentially any frequency to which the absorber is tuned, without generating
unwanted peaks. In fact, the absorber system behaves as a mechanical "notch
filter" capable of providing a high degree of isolation at a single frequency.
Hence, the system may be used with advantage to protect delicate instrumen-
tation, for example, from troublesome foundation vibrations occurring at
discrete "low" frequencies.

The resonant vibration of distributed mechanical systems such as beams
and plates can also be reduced effectively by the attachment of dynamic

absorbers of appropriate design. As an example, dual dynamic absorbers applied to reduce the force transmissibility at resonance across an undamped cantilever beam are shown in Figure 27. The absorber at the free end of the beam is tuned to suppress the fundamental beam resonance while the central absorber is tuned to suppress the second beam resonance. The force transmissibility $T = |\tilde{F}_T/\tilde{F}_O|$ across the unloaded beam is shown as the dashed-line curve in Figure 28. Transmissibility is plotted in terms of the product of the beam length ℓ and a parameter n, which is proportional to the square root of frequency. The parameter n, the beam wavenumber, is defined by the equation

$$n^4 = \omega^2 \rho / r^2 E \ ,$$

where ρ and E are the density and Young's modulus of the beam material, and r is the radius of gyration of the beam cross section.

The effectiveness of dynamic absorbers of optimum design in reducing the transmissibility across the beam is typified by the solid-line curve of Figure 28. In this example, the masses of the absorbers at the free end and center of the beam (25% and 10% of the beam mass, respectively) are so chosen that the first two transmissibility peaks are equally suppressed to a value slightly greater than 2. Had absorbers with only 5% and 2.5% of the beam mass been utilized, this value would be slightly greater than 5.

Dynamic absorbers are very effective in suppressing the resonant vibration of plates. Thus, Figure 29 shows a dynamic absorber attached to the center of a circular plate such as a bulkhead, which is clamped around its boundary. The plate has internal damping factors of 0.01, which are sufficiently small that the force transmissibility across the plate -- namely, the output ring of force $\tilde{F}_1$ divided by the impressed force $\tilde{F}_O$ -- becomes

untenably large at the plate resonances unless the dynamic absorber is utilized. Calculations of transmissibility are plotted in Figure 30 on a scale that is again proportional to $\sqrt{\omega}$. The dashed-line curve shows the transmissibility across the plate in the absence of the absorber. The first peak corresponds to a maximum transmissibility of 150 at the fundamental plate resonance. A dynamic absorber having 10 or 25% of the plate mass, and having optimum tuning and damping, is seen to suppress this peak to a maximum value of slightly more than 3 or 2, respectively. Note that the absorber damping is effective also in suppressing the second and third plate resonances at higher frequencies. Thus, the absorber mass remains almost stationary at frequencies above its own resonance, providing a "fixed" point from which the absorber dashpot can restrain the motion of the plate at resonance, and the corresponding force transmissibility to the plate boundaries.

It is of interest now to examine an absorber of somewhat different design, as shown in Figure 31. The so-called platelike absorber of Figure 31(a) is essentially as effective as a conventional absorber and yet it possesses the advantages of mechanical simplicity and planar geometry for compact flush-mounted application on panels and bulkheads, or beneath the floors and seats of the crew compartments in a ship or flight vehicle, for example. The absorber comprises a damped circular steel plate that is loaded at its midpoint by a lumped mass, which is always assumed to be five times greater than the plate mass. The plate, which acts as a combined spring and damper, is clamped around its perimeter where it is rigidly connected to the vibrating item or structure of concern. The plate could either be coated with damping compound, or could be made from steel/viscoelastic laminations. Such laminates can be produced with the relatively high damping factors needed in most absorber applications.

Representative calculations of the transmissibility across the undamped primary system of Figure 31(b) that has mass M_1 and stiffness K_1 are plotted in Figure 32 for attached dynamic absorbers that are 1/50, 1/10, and 1/2 as large as M_1. Note that, because of appropriate absorber design, the transmissibility in each case is suppressed effectively and symmetrically about the dashed-line curve, which shows the undamped transmissibility at resonance of the primary system alone.

To conclude, it is instructive to point out that the transient performance of the dynamic absorber is also excellent. Refer again to Figure 20, which shows an undamped primary system of mass M_1, on this occasion subjected to a transient input displacement $x_1(t)$, where t is time. A dynamic absorber of optimum design for sinusoidal vibration is attached to M_1, which experiences a transient displacement $x_2(t)$. The input displacement $x_1(t)$ is assumed to be a series of step functions that have a finite rise time, as shown in Figure 33. The input displacement $x_1(t)$ is normalized here by division by its maximum value x_{max}. Choice of a parameter γ changes the input from a very gradual ramplike step when γ is small to an abrupt almost right-angled step when γ is large. In fact, γ is defined as follows:

$$\gamma = \pi/\omega_o \tau \ ,$$

where τ is the step "rise time" required for the displacements $x_1(t)$ to reach 82% of their final amplitude x_{max}. The response of the mounting system to this series of displacements is shown in the final Figure 34. Here, the resultant acceleration $\ddot{x}_2/\omega_o^2 x_{max}$, displacement x_2/x_{max}, and relative displacement $(x_2 - x_1)/x_{max}$ of M_1 are plotted on the same time scale as in Figure 33. The dynamic absorber has one-fifth of the mass M_1. The chain-line curves describe the response of a damped simple system (dynamic absorber

absent) to a discontinuous displacement step for which $\gamma \to \infty$. The chain-line curve for displacement has been made to coincide with the maximum absorber displacement induced by the rounded step input for which $\gamma = 50$.

Reference to Figure 34 shows that use of the dynamic absorber (1) has yielded a low maximum acceleration of M_1, which will reduce the likelihood of damage to those fragile items within M_1 that have high natural frequencies, and (2) -- of tangible benefit -- has yielded an oscillatory transient motion of M_1 that decays with time far more rapidly than the motion of the simple system alone. And so, it follows that not only will the dynamic absorber reduce the risk of failure from fatigue of fragile elements within M_1, but that it will also facilitate the reading of any meters, gages, etc., that are attached to M_1, particularly if the transient disturbances are repetitive.

BIBLIOGRAPHY

1. E. G. Fischer and H. M. Forkois, contribution to Shock and Vibration Handbook, edited by C. M. Harris and C. E. Crede (McGraw-Hill Book Company, Inc., New York, 1961), Chap. 43, pp. 43.1-43.40.

2. R. M. Gorman, Shock and Vib. Bull. 35, Pt. 5, 227 (1966).

3. D. I. G. Jones, A. D. Nashif, R. L. Adkins, J. AIAA 5, 310 (1967).

4. J. J. Sciarra, Am. Soc. Mech. Engrs. Reprint No. 67-VIBR-65 (1967).

5. J. C. Snowdon

    (a) Vibration and Shock in Damped Mechanical Systems (John Wiley and Sons, Inc., New York, 1968).

    (b) J. Sound. Vib. 15, 307 (1971).

    (c) Acustica 28, 307 (1973).

    (d) J. Soc. Environ. Engrs. 12, No. 3, 2 (1973).

    (e) Contribution to Isolation of Mechanical Vibration, Impact, and Noise, edited by J. C. Snowdon and E. E. Ungar (American Society of Mechanical Engineers, New York, 1973), Chap. 5, pp. 102-127.

FIGURE LEGENDS

Fig. 1   Simple mounting system with a machine (a) supported directly, and (b) supported by nonrigid flanges or feet.

Fig. 2   Force transmissibility across the simple mounting system of Figure 1(a).

Fig. 3   Force transmissibility across the simple mounting system of Figure 1(b). Machine feet-to-mount stiffness ratio Γ = 5, 25, and 100.

Fig. 4   Marine engine supported by a resiliently mounted subframe.

Fig. 5   Axial-flow fan supported by a resiliently mounted subframe.

Fig. 6   Compound mounting system with a machine and an intermediate or secondary mass, which is supported (a) directly, and (b) via nonrigid flanges or feet.

Fig. 7   Force transmissibility across the compound system of Figure 6(a) employing natural-rubber mounts. Mass ratio $\beta = M_2/M_1$ = 0.1, 0.2, and 1.0.

Fig. 8   Example of a small-scale application of the compound system.

Fig. 9   Example of a large-scale application of the compound system.

Fig. 10   Force transmissibility across the compound systems of Figure 6(a) (solid-line curve) and Figure 6(b) (chain-line curve). Mass ratio β = 0.2.

Fig. 11   Simple mounting system with nonrigid foundations modeled (a) by a clamped-clamped beam and (b) by a simply supported plate.

Fig. 12   Force transmissibility across a mounting system with a machine supported by one mount as in Figure 11(a) (solid-line curve), or by eight mounts spaced at equal intervals along the beam, as in Figure 13 (chain-line curve).

Fig. 23   Transmissibility of the viscously damped dynamic absorber of Figure 20. Optimum absorber tuning and damping for the mass ratios μ = 50/51, 10/11, 5/6, and 1/2.

Fig. 24   Example of a small-scale application of the dynamic absorber.

Fig. 25   Example of a large-scale application of the dynamic absorber.

Fig. 26   Transmissibility of the dynamic absorber of Figure 20 tuned three frequencies in turn. Primary system has one-half critical viscous damping. Absorber is lightly damped and has a mass ratio μ = 5/6.

Fig. 27   Dynamic absorbers attached to the free end and to the midpoint of an undamped cantilever beam.

Fig. 28   Force transmissibility across the cantilever beam of Figure 27; optimum absorber tuning and damping for values of the mass ratios μ = 4/5 and 10/11 $[\mu = (1 + \gamma_a)^{-1}]$.

Fig. 29   Dynamic absorber attached to the midpoint of a centrally driven clamped circular plate.

Fig. 30   Force transmissibility across the circular plate of Figure 29; optimum absorber tuning and damping for values of the mass ratios μ = 4/5 and 10/11 $[\mu = (1 + \gamma_a)^{-1}]$.

Fig. 31   (a) Section through a circular platelike dynamic absorber, and (b) a circular platelike absorber attached to an undamped primary system.

Fig. 32   Force transmissibility of the platelike dynamic absorber of Figure 31. Optimum absorber tuning and damping for the mass ratios μ = 50/51, 10/11, and 2/3.

Fig. 33   Series of rounded step displacements.

Fig. 34   Acceleration-, displacement-, and relative displacement-time
curves for the dynamic absorber of Figure 20 subjected to the
rounded step displacements of Figure 33.   Optimum tuning and
damping for the absorber mass ratio μ = 5/6.

(a)

(b)
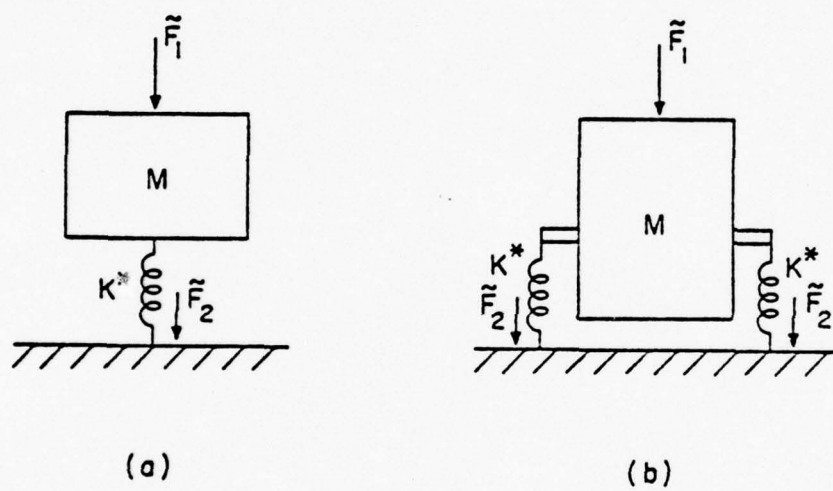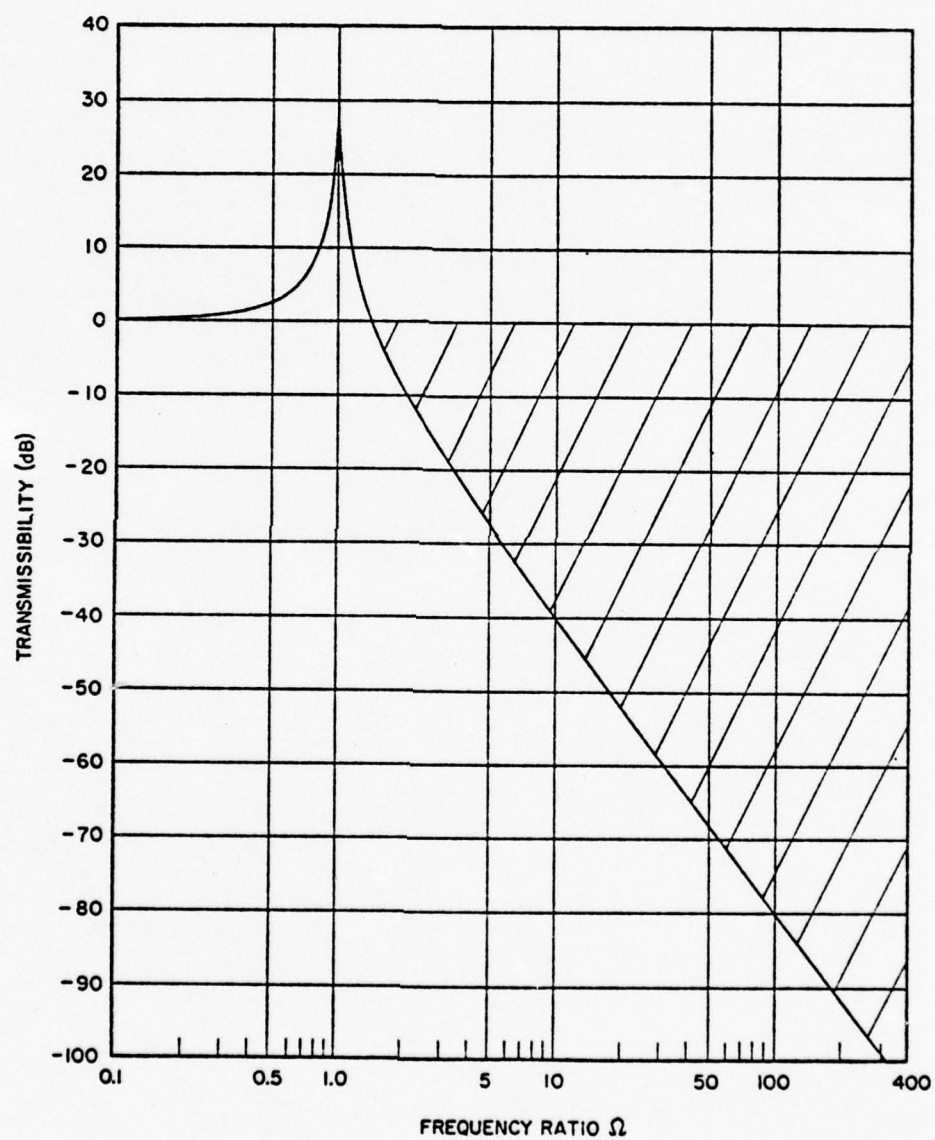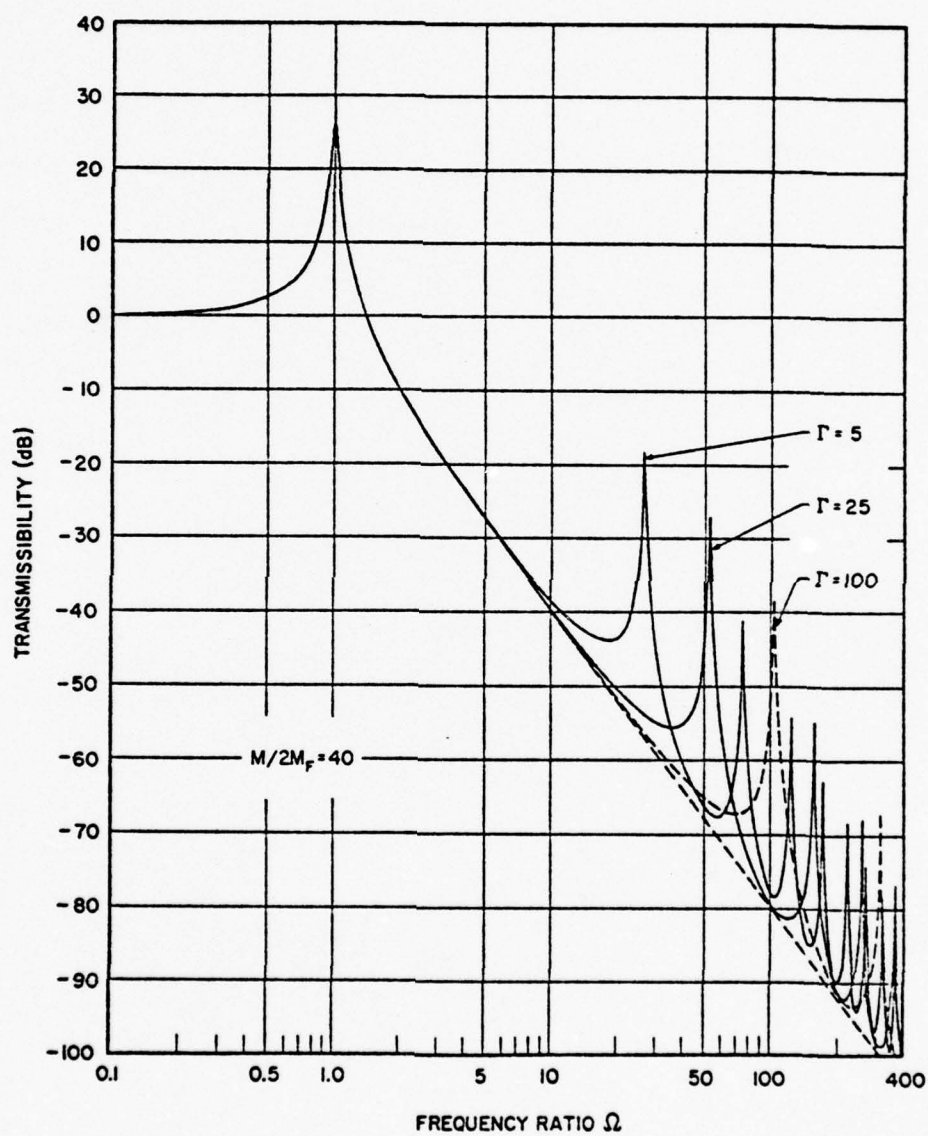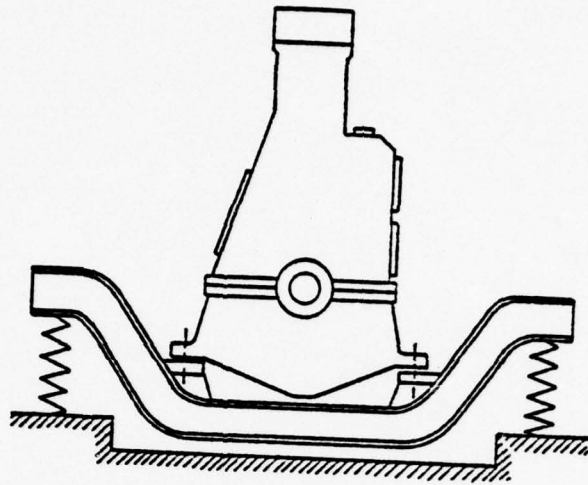
Fig. 1

Fig. 2

Fig. 3

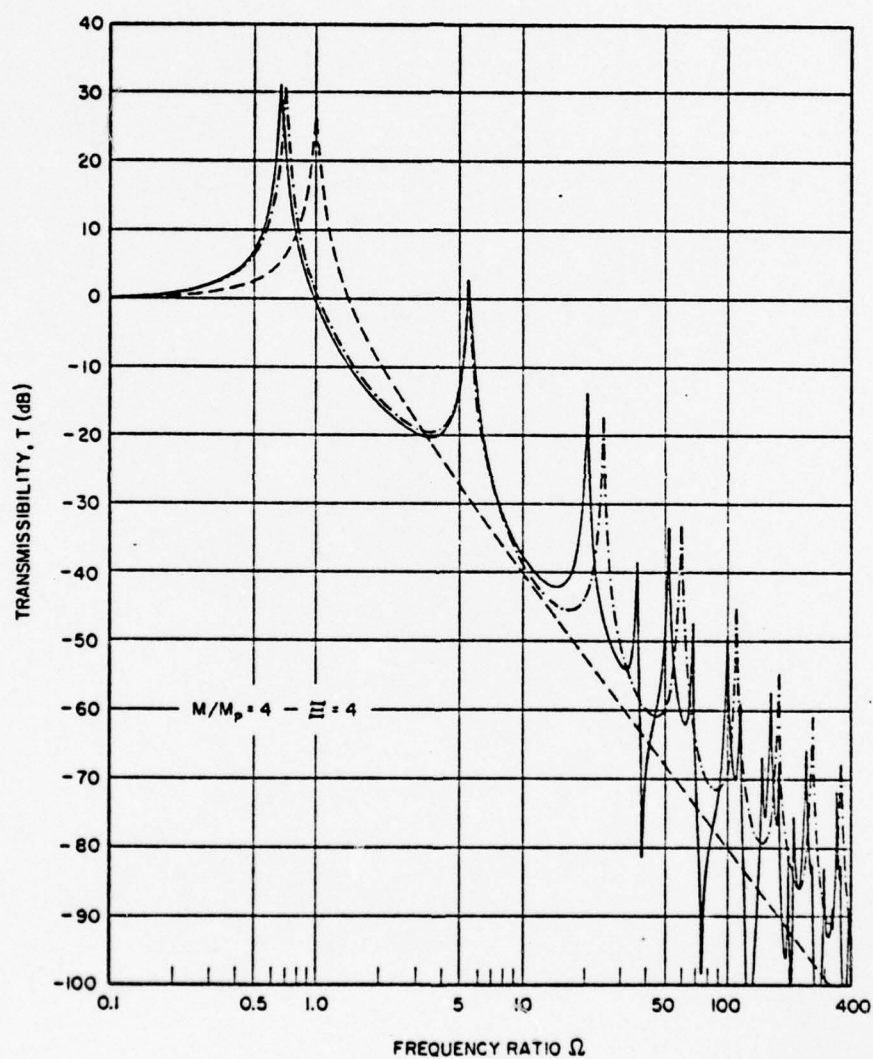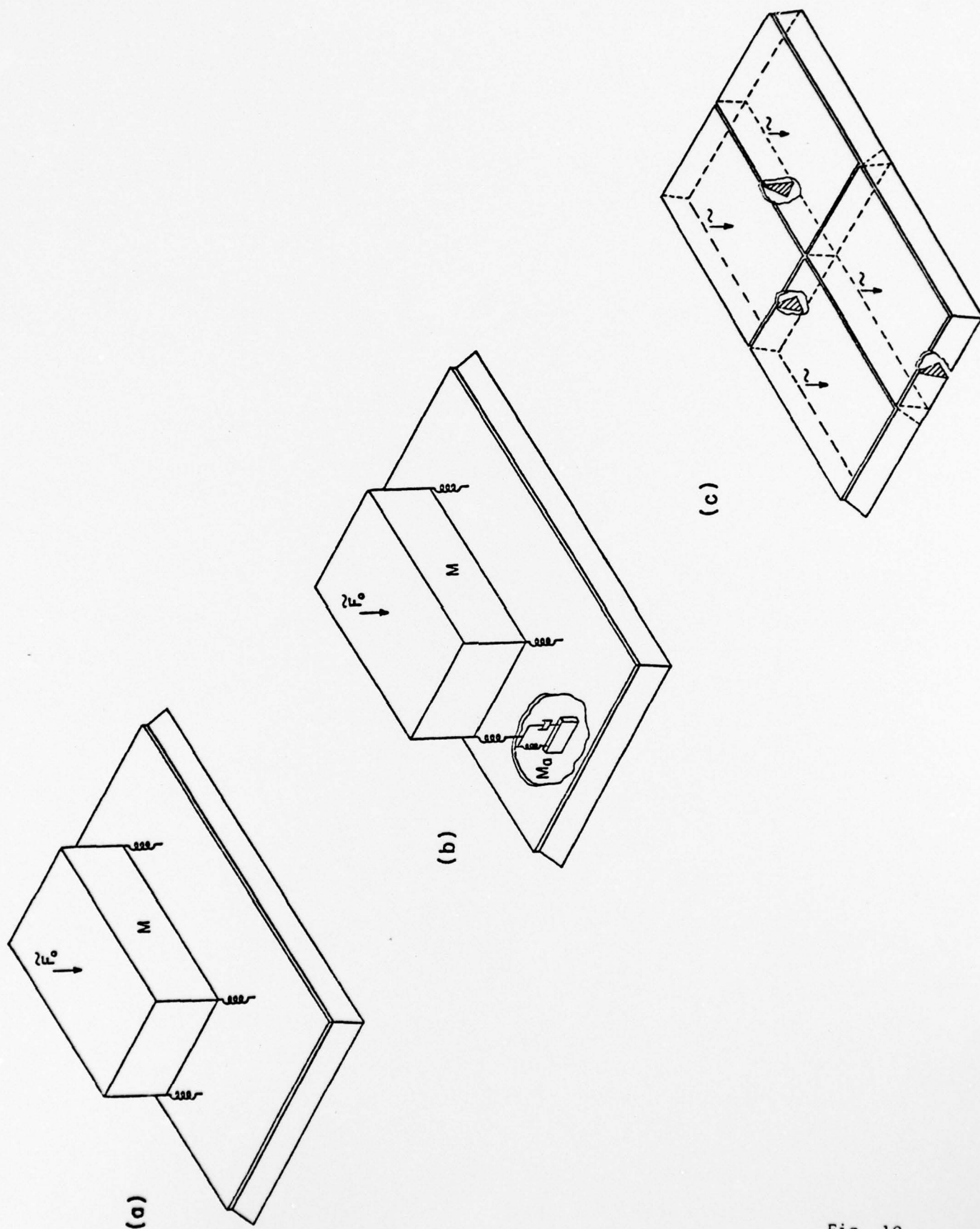Fig. 4
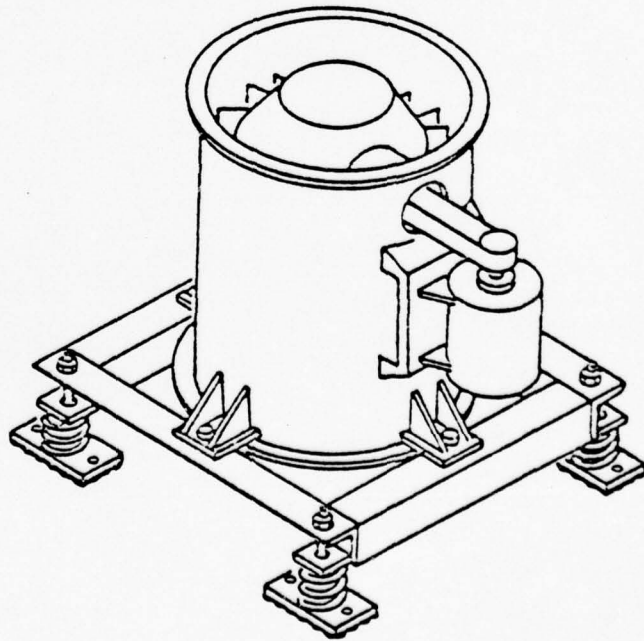
Fig. 5
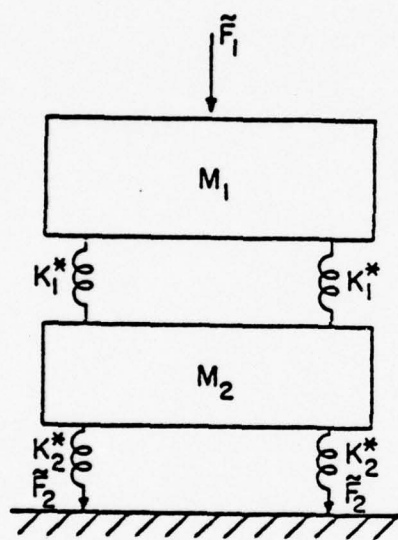
(a)
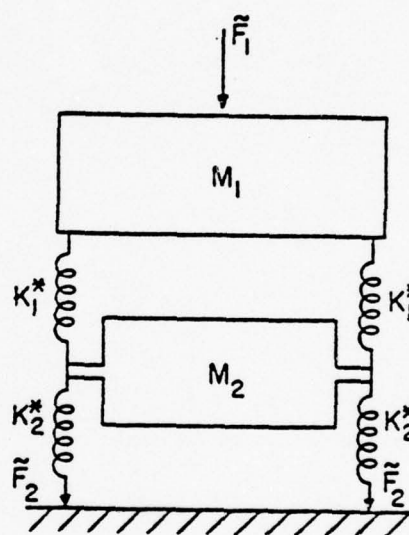
(b)

Fig. 6
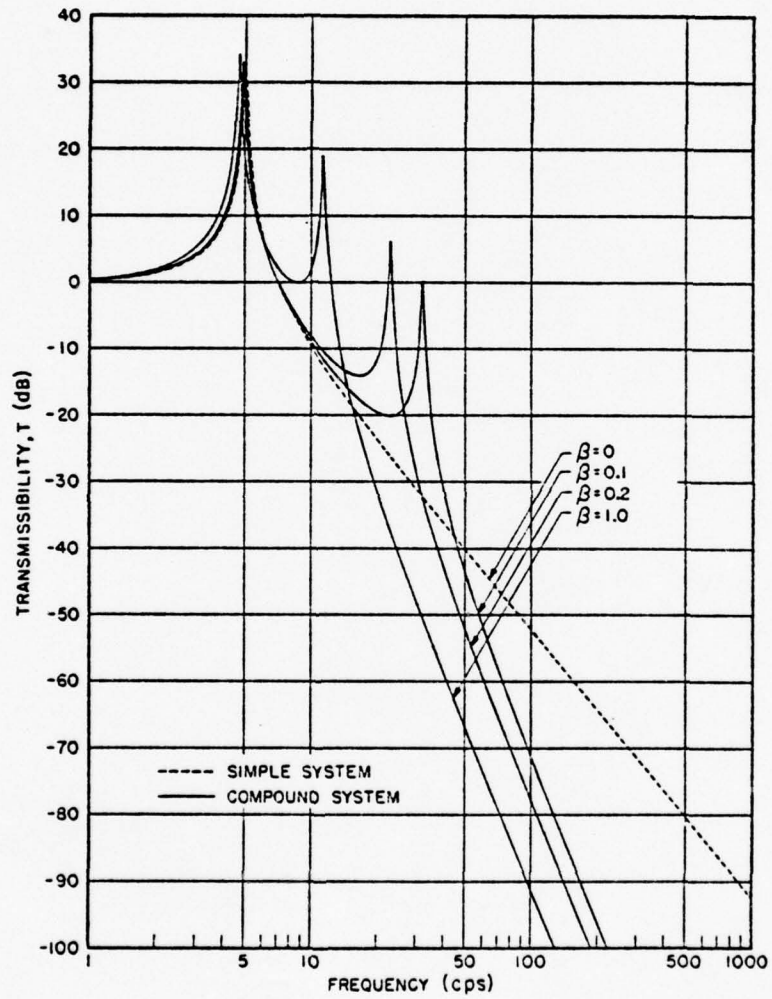
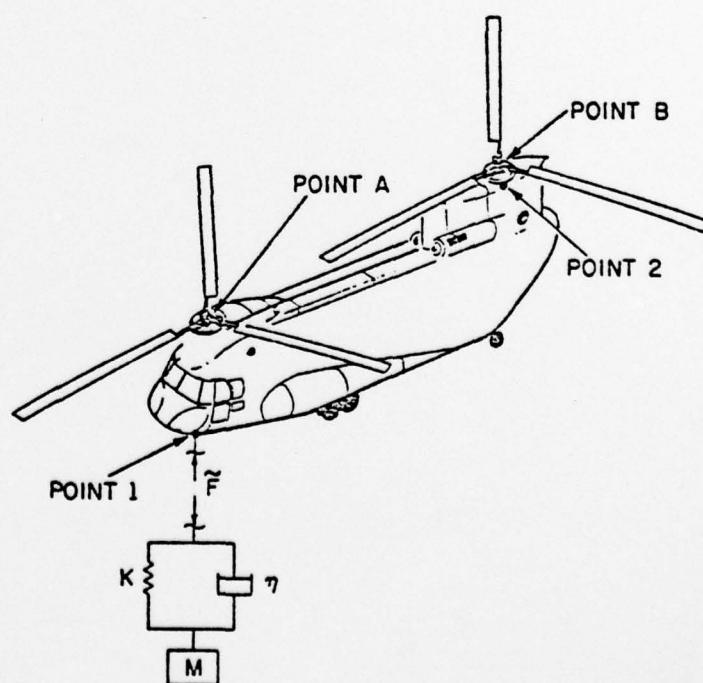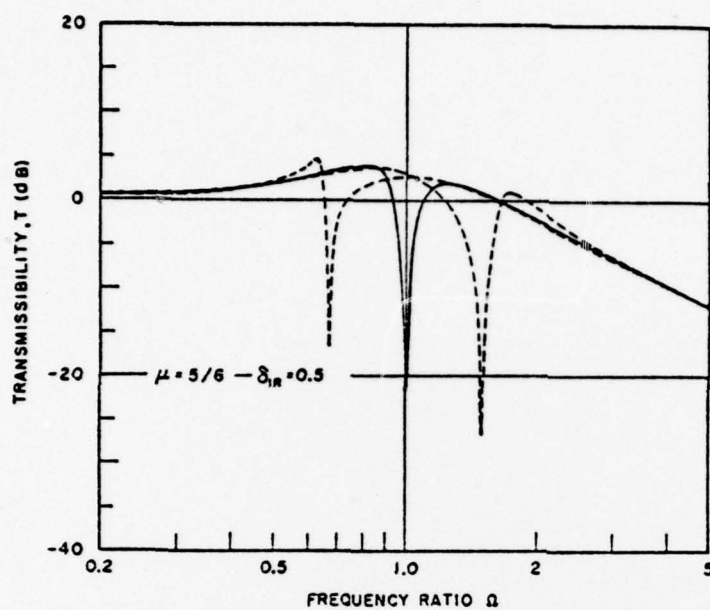Fig. 7
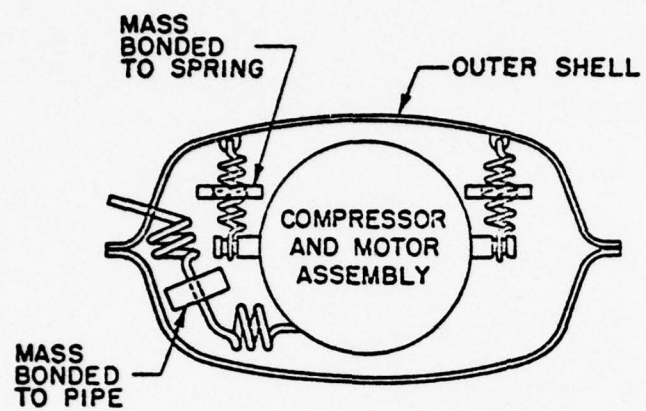
Fig. 8
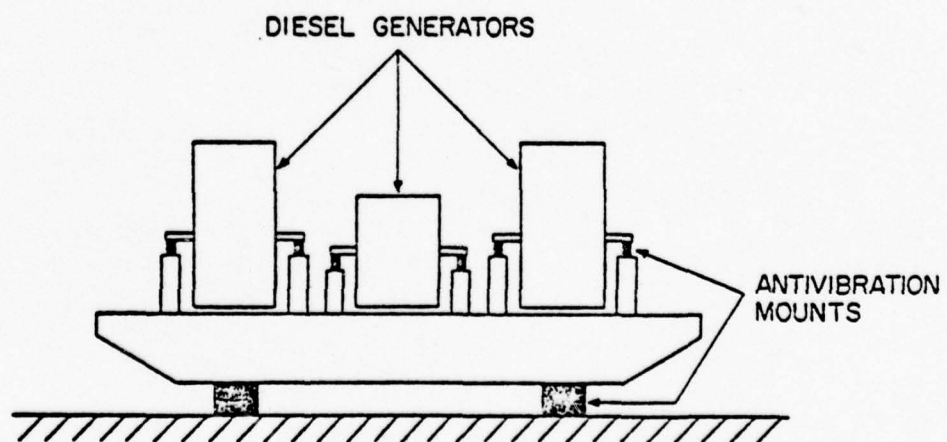
Fig. 9
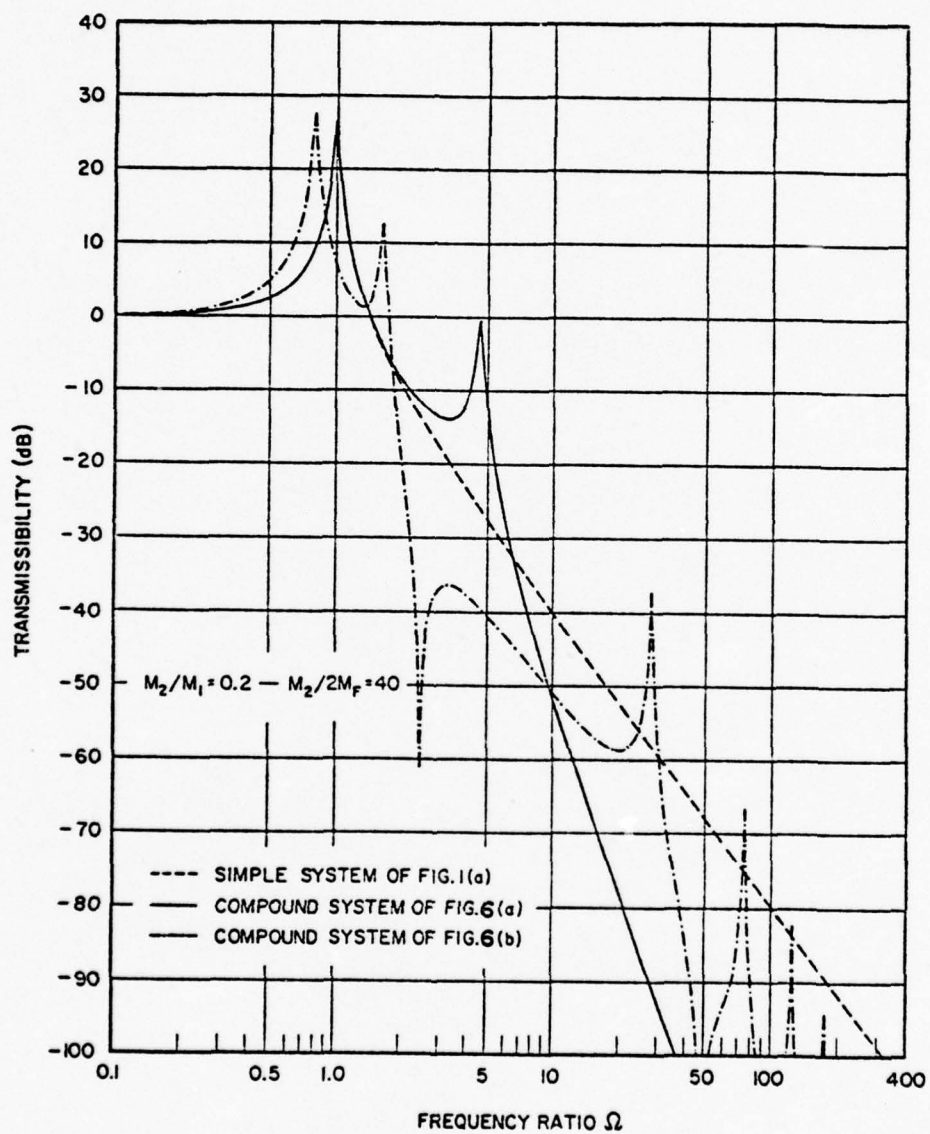
Fig. 10
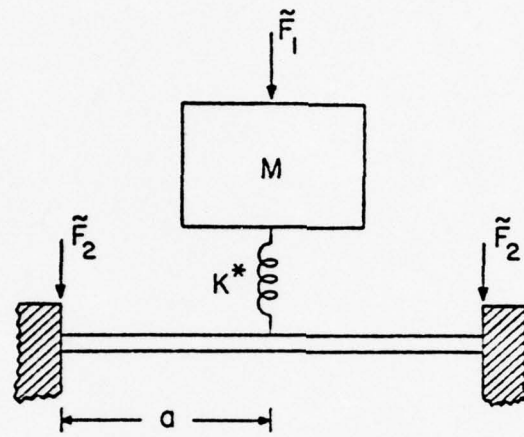
(a)
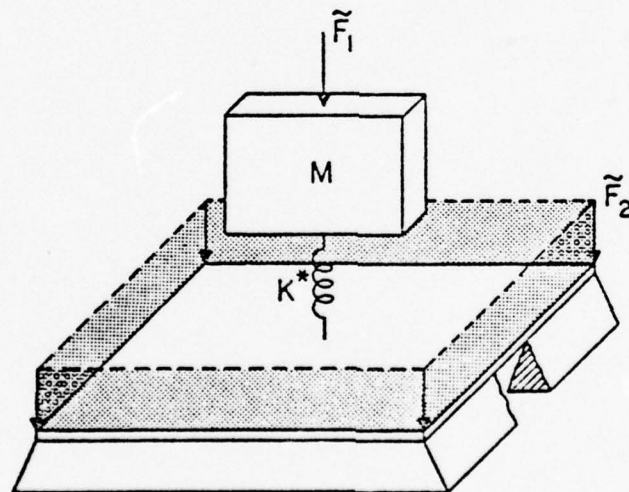
(b)

Fig. 11
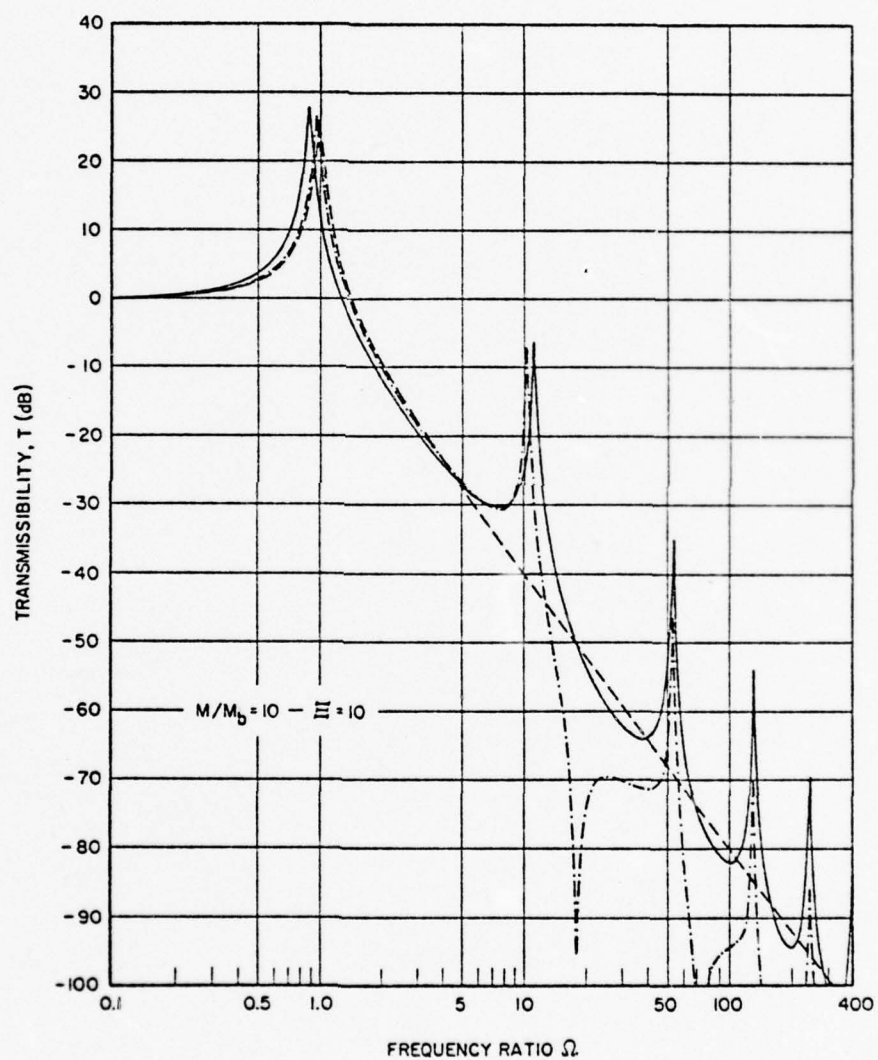
Fig. 12
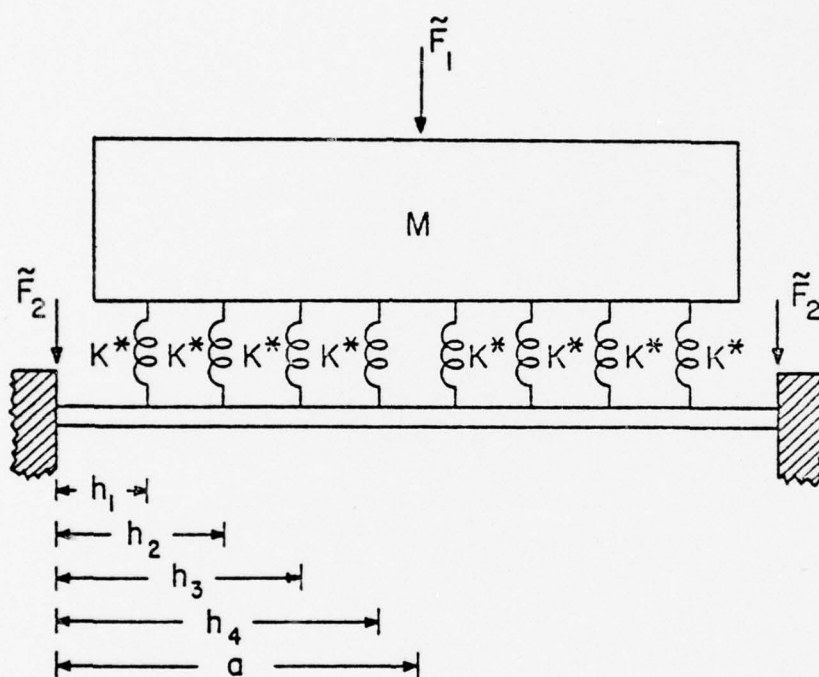
Fig.`13
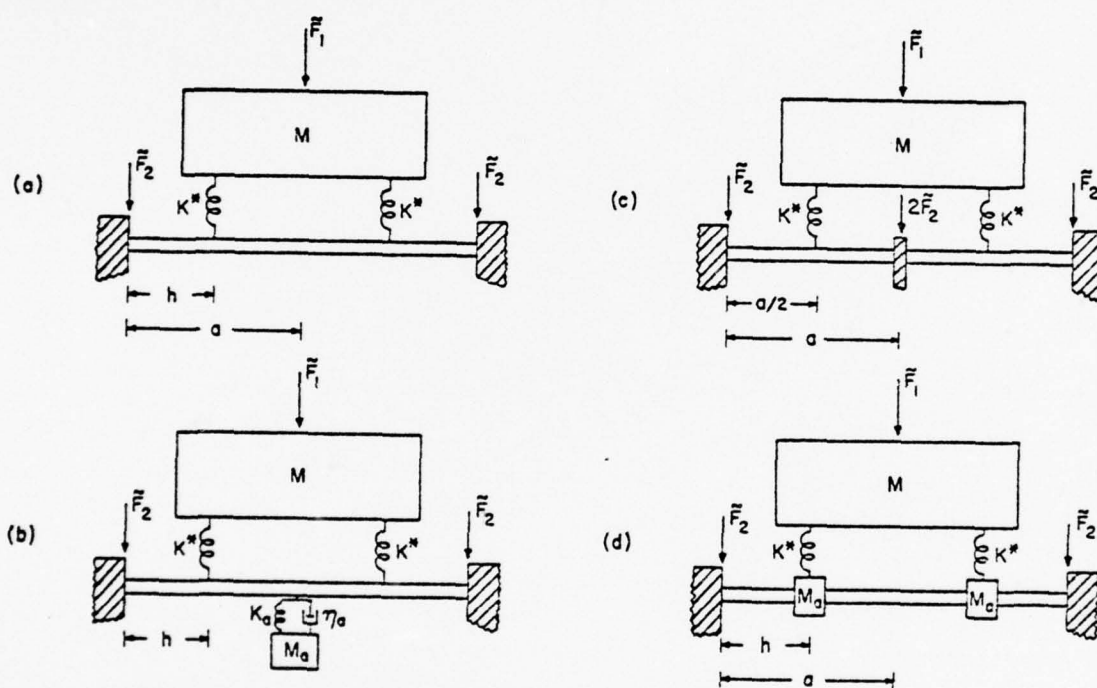
Fig. 14
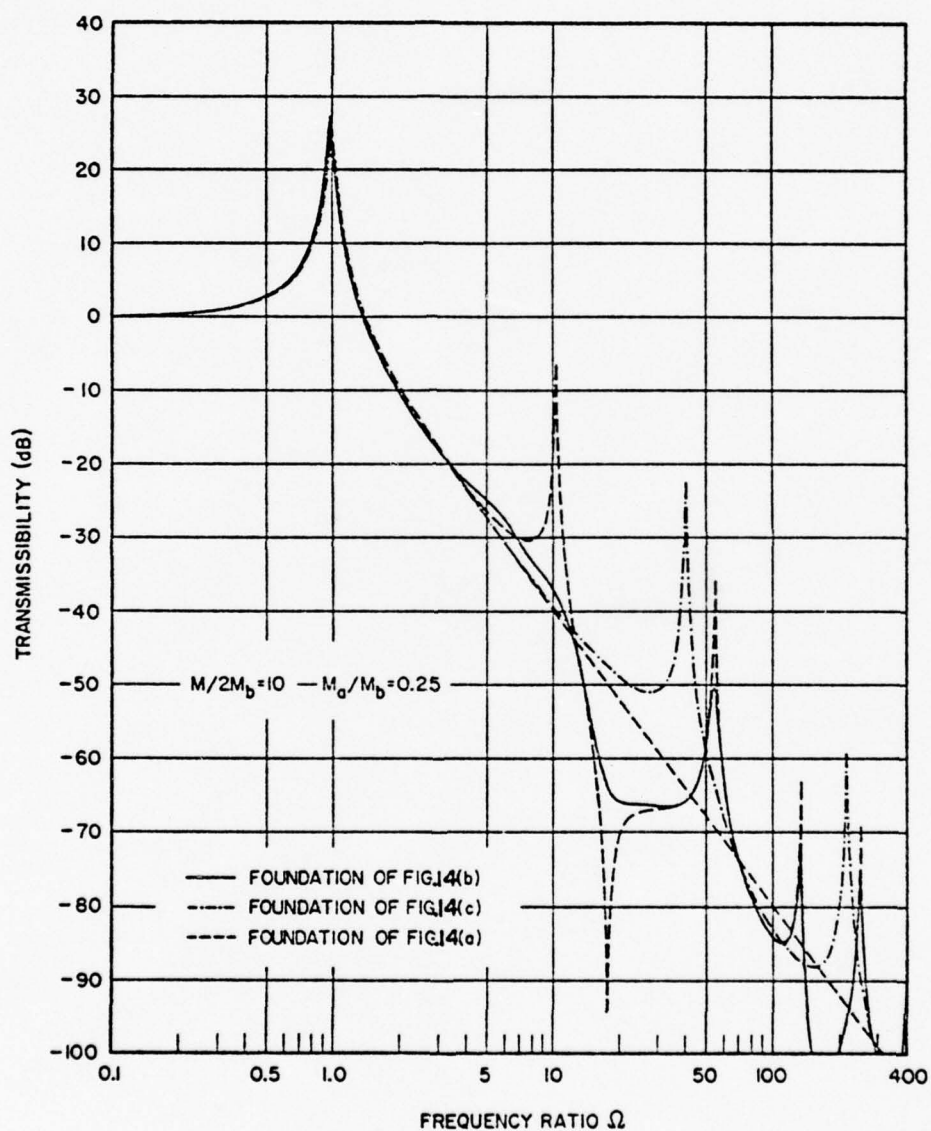
Fig. 15

Fig. 16

Fig. 17

Fig. 18

(a)

(b)

(c)
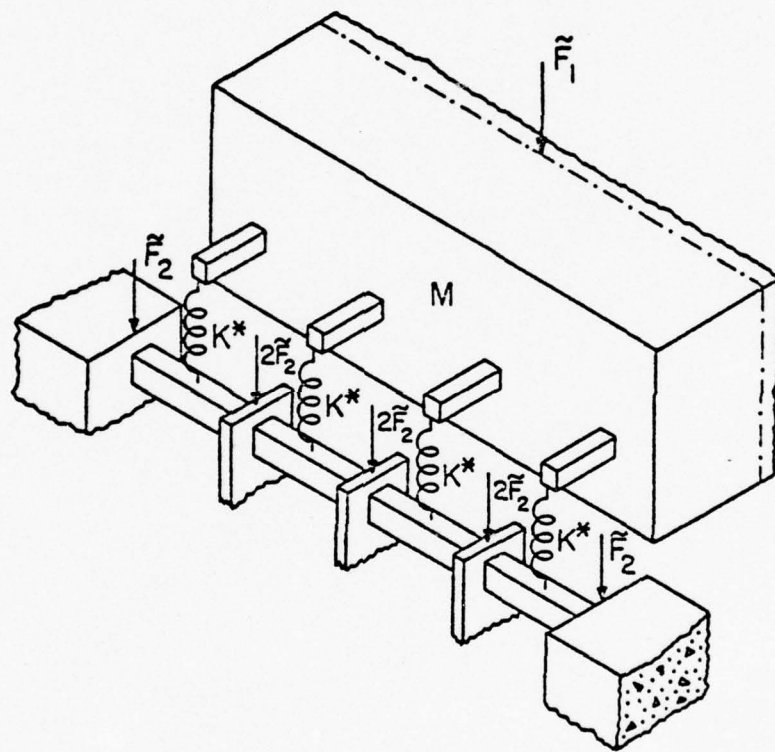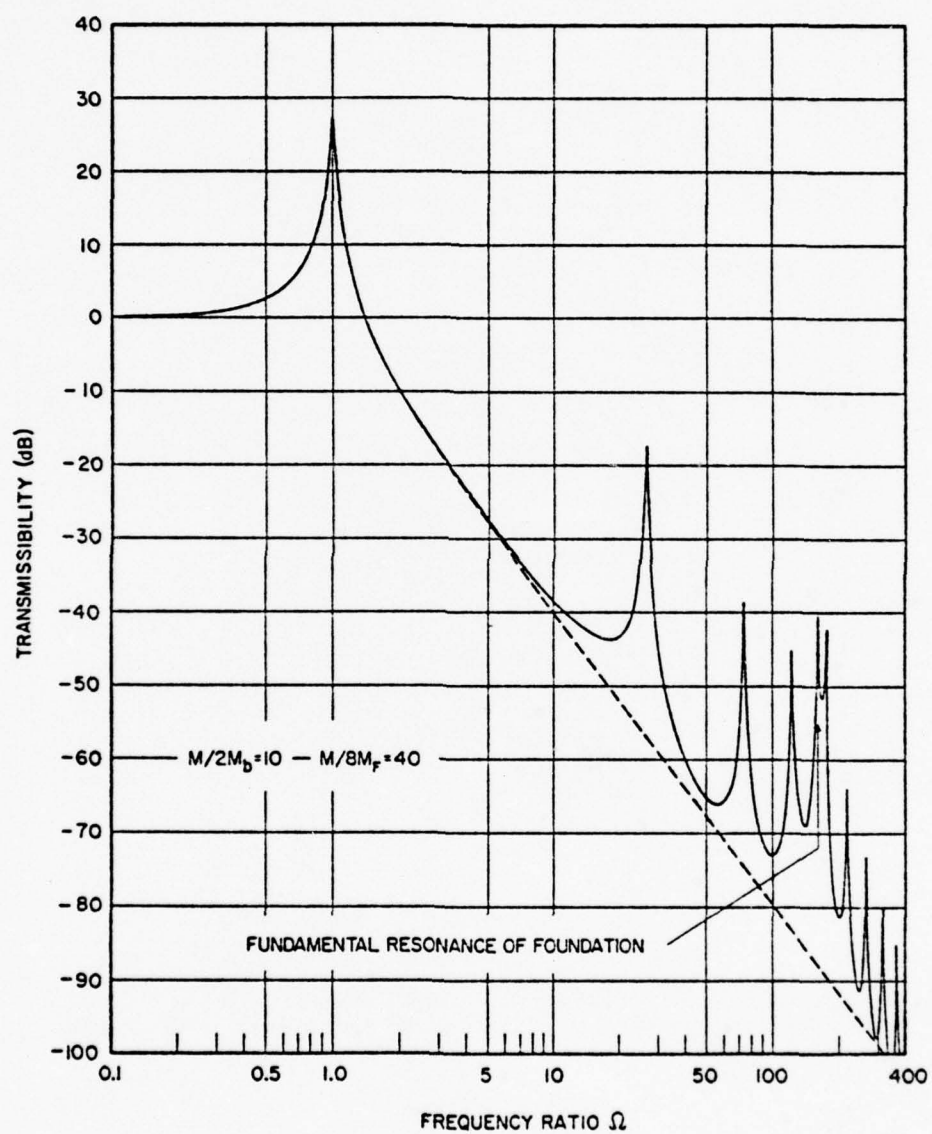
Fig. 19
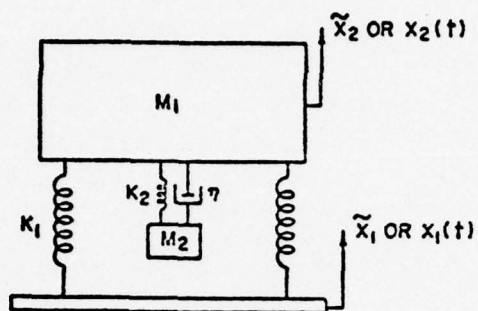
Fig. 20
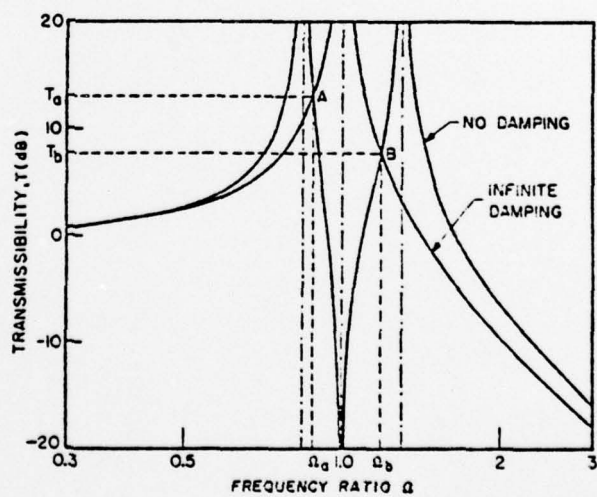
Fig. 21
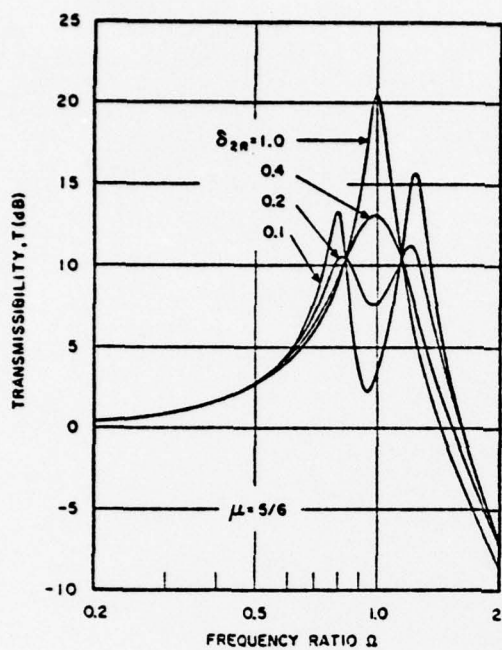
Fig. 22
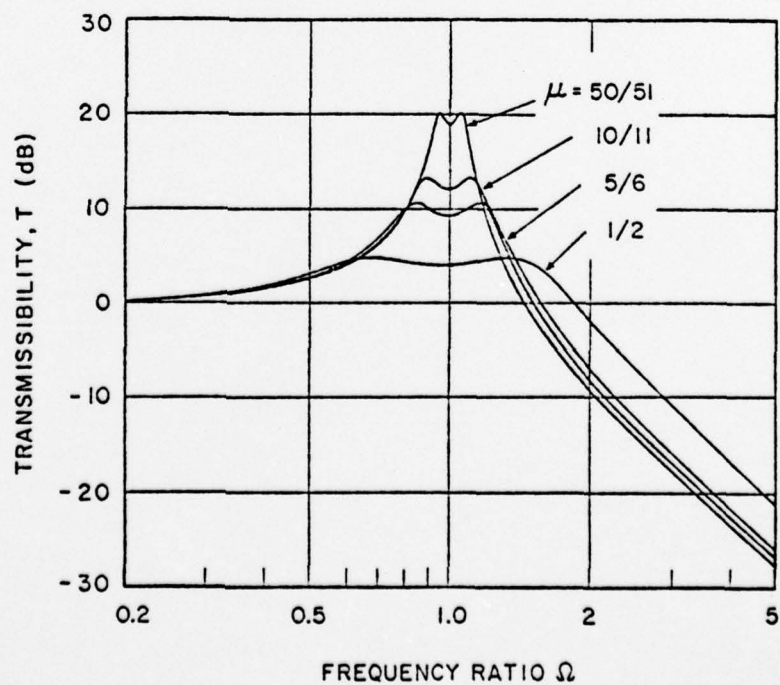
Fig. 23
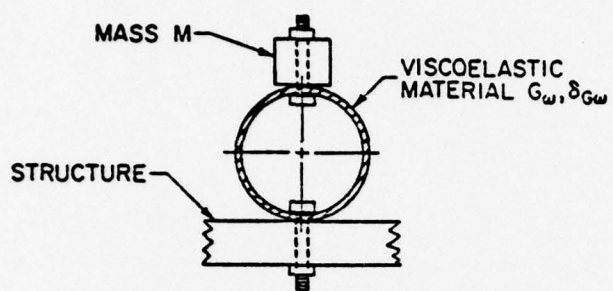
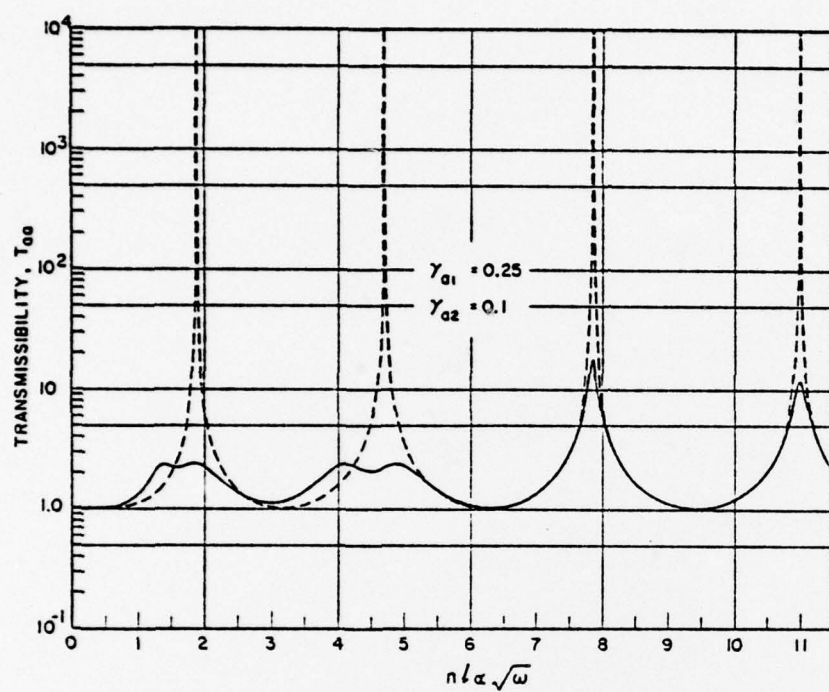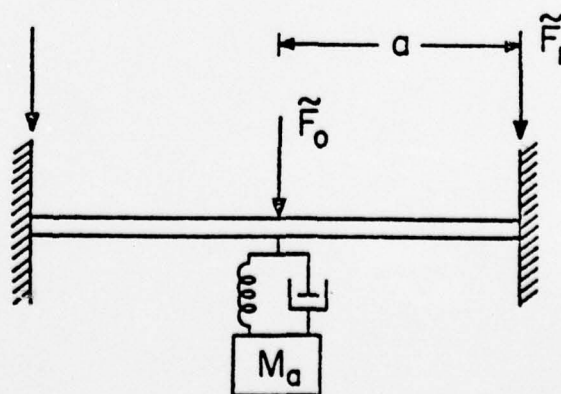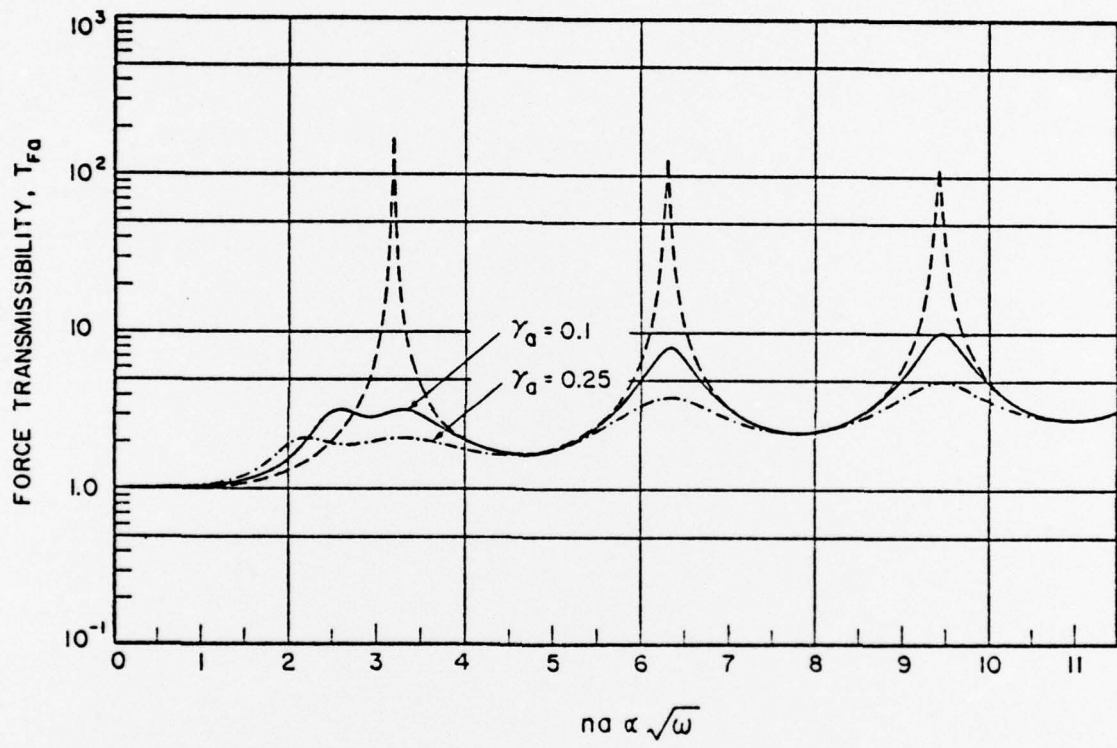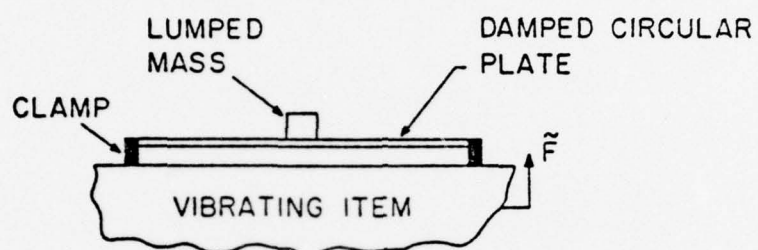RING DAMPER AT CENTER OF PANEL OR BEAM

Fig. 24

Fig. 25

Fig. 26
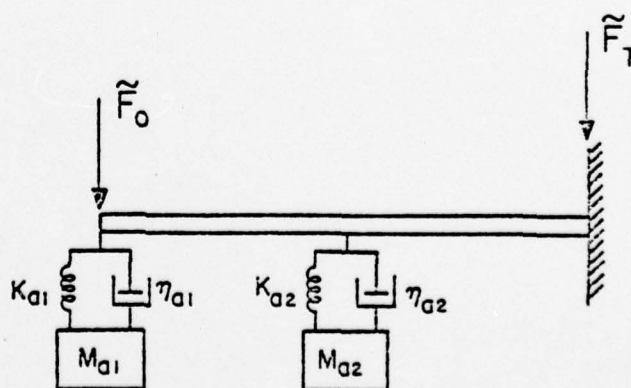
Fig. 27

Fig. 28

Fig. 29
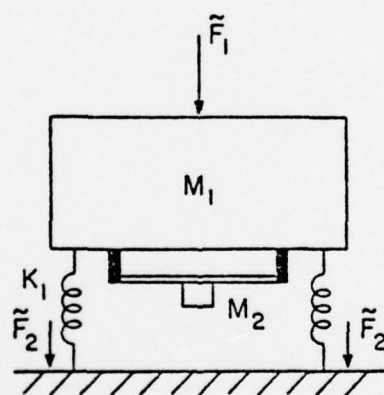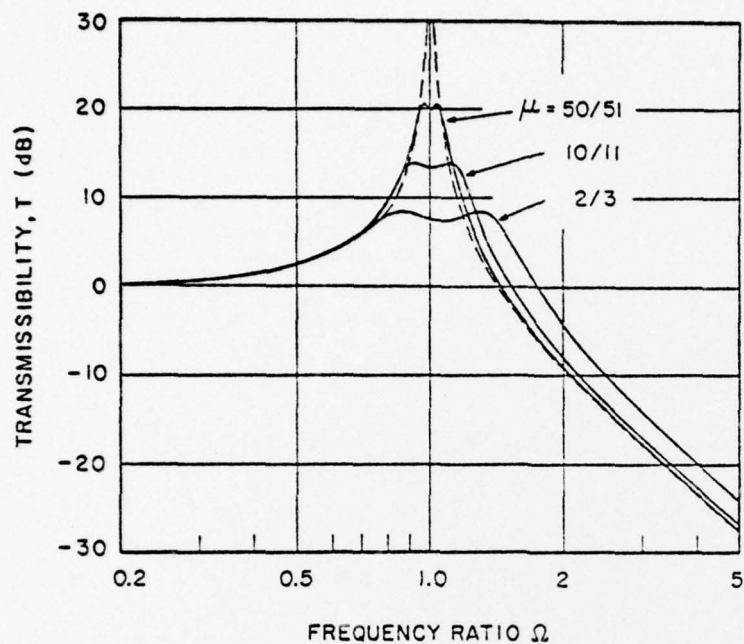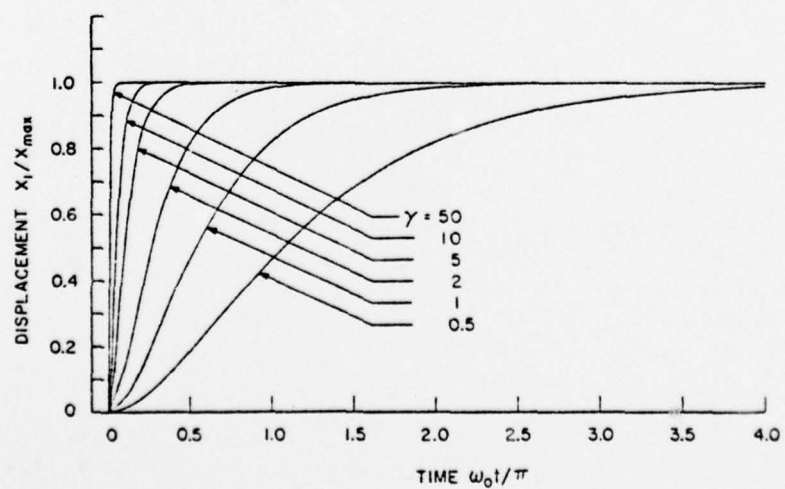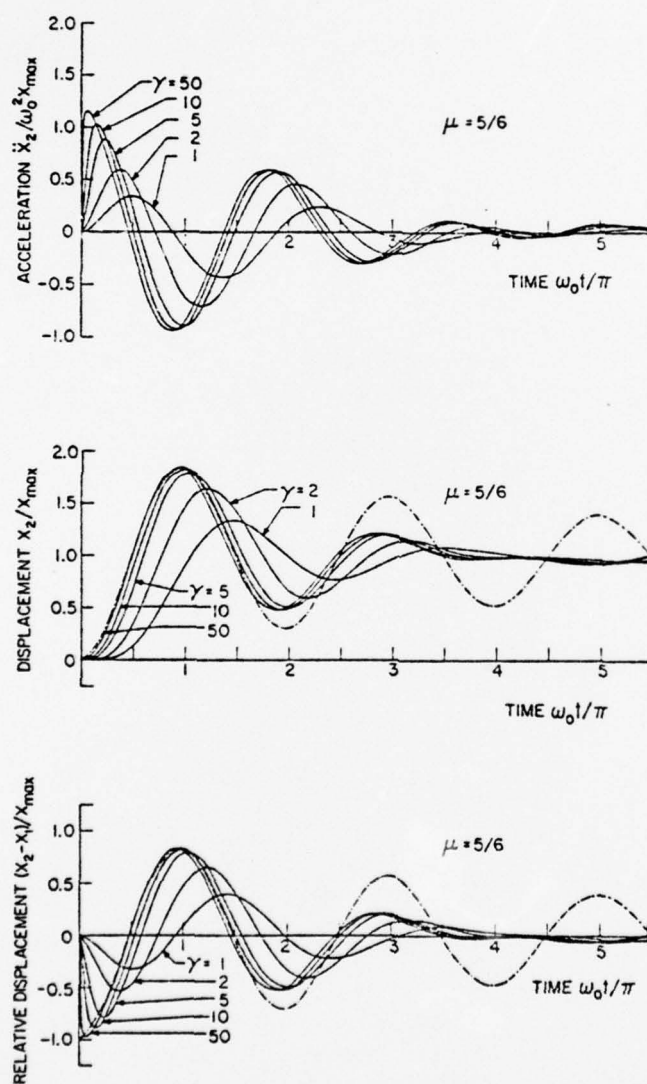
Fig. 30

Fig. 31

Fig. 32

Fig. 33

Fig. 34

DISTRIBUTION LIST FOR UNCLASSIFIED TM 76-188

Commander
Naval Sea Systems Command
Department of the Navy
Washington, DC 20362
Attn: SEA 924N
(Copy No. 1)

Commander
Naval Sea Systems Command
Department of the Navy
Washington, DC 20362
Attn: PMS-393
(Copy No. 2)

Commander
Naval Sea Systems Command
Department of the Navy
Washington, DC 20362
Attn: PMS-395
(Copy No. 3)

Commander
Naval Sea Systems Command
Department of the Navy
Washington, DC 20362
Attn: PMS-396
(Copy No. 4)

Commander
Naval Sea Systems Command
Department of the Navy
Washington, DC 20362
Attn: Mr. Stephen M. Blazek
SEA 0371
(Copy Nos. 5, 6, 7, 8)

Commander
Naval Sea Systems Command
Department of the Navy
Washington, DC 20362
Attn: Mr. Stephen G. Wieczorek
SEA 037T
(Copy Nos. 9 and 10)

Commander
Naval Sea Systems Command
Department of the Navy
Washington, DC 20362
Attn: Mr. C. C. Taylor
SEA 0372
(Copy Nos. 11 and 12)

Commander
Naval Ship Engineering Center
Center Building
Prince George's Center
Hyattsville, MD 20782
Attn: NAVSEC 6103E
(Copy Nos. 13 and 14)

Commander
Naval Ship Engineering Center
Center Building
Prince George's Center
Hyattsville, MD 20782
Attn: NAVSEC 6105C
(Copy Nos. 15 and 16)

Commander
Naval Ship Engineering Center
Center Building
Prince George's Center
Hyattsville, MD 20782
Attn: Mr. Kenneth G. Hartman
NAVSEC 6105N
(Copy Nos. 17, 18, 19, 20, 21, 22)

Commander
Naval Ship Engineering Center
Center Building
Prince George's Center
Hyattsville, MD 20782
Attn: NAVSEC 6111B
(Copy Nos. 23 and 24)

Commander
Naval Ship Engineering Center
Center Building
Prince George's Center
Hyattsville, MD 20782
Attn: NAVSEC 6111D
(Copy Nos. 25 and 26)

Commander
Naval Ship Engineering Center
Center Building
Prince George's Center
Hyattsville, MD 20782
Attn: NAVSEC 6113C
(Copy Nos. 27 and 28)

Commander
Naval Ship Engineering Center
Center Building
Prince George's Center
Hyattsville, MD 20782
Attn: NAVSEC 6113D
(Copy Nos. 29 and 30)

Commander
Naval Ship Engineering Center
Center Building
Prince George's Center
Hyattsville, MD 20782
Attn: NAVSEC 6120
(Copy Nos. 31 and 32)

Commander
Naval Ship Engineering Center
Center Building
Prince George's Center
Hyattsville, MD 20782
Attn: NAVSEC 6129
(Copy Nos. 33 and 34)

Naval Ship Research and Development Center
Annapolis Division
Annapolis, MD 21402
Attn: Mr. J. Smith
(Copy No. 35)

Naval Ship Research and Development Center
Annapolis Division
Annapolis, MD 21402
Attn: Mr. L. J. Argiro
(Copy Nos. 36, 37, 38, 39, 40, 41)

Naval Ship Research and Development Center
Bethesda, MD 20084
Attn: Dr. M. Sevik
Code 19
(Copy Nos. 42 and 43)

Naval Ship Research and Development Center
Bethesda, MD 20084
Attn: Dr. W. W. Murray
Code 17
(Copy Nos. 44 and 45)

Naval Ship Research and Development Center
Bethesda, MD 20084
Attn: Dr. M. Strasberg
Code 1901
(Copy No. 46)

Naval Ship Research and Development Center
Bethesda, MD 20084
Attn: Dr. G. Maidanik
Code 1902
(Copy No. 47)

Naval Ship Research and Development Center
Bethesda, MD 20084
Attn: Dr. G. Chertock
Code 1903
(Copy No. 48)

Naval Ship Research and Development Center
Bethesda, MD 20084
Attn: Dr. D. Feit
Code 196
(Copy Nos. 49, 50, 51, 52, 53, 54)

Naval Ship Research and Development Center
Bethesda, MD 20084
Attn: Dr. J. T. Shen
Code 1942
(Copy No. 55)

Director
Defense Documentation Center
Cameron Station
Alexandria, VA 22314
(Copy Nos. 56, 57, 58, 59, 60, 61,
62, 63, 64, 65, 66, 67)

Director
Naval Research Laboratory
Washington, DC 20390
Attn: Code 8440
(Copy Nos. 68 and 69)

Ocean Structures Branch
U. S. Naval Research Laboratory
Washington, DC 20390
Attn: Dr. R. O. Belsheim
(Copy No. 70)

Office of Naval Research
Department of the Navy
Arlington, VA 22217
Attn: Dr. G. Boyer
Code 222
(Copy Nos. 71, 72, 73)

Office of Naval Research
Department of the Navy
Arlington, VA 22217
Attn: Dr. A. O. Sykes
        Code 222
(Copy Nos. 74, 75, 76)

Office of Naval Research
Department of the Navy
Arlington, VA 22217
Attn: Mr. Keith M. Ellingsworth
        Code 473
(Copy No. 77)

Office of Naval Research
Department of the Navy
Arlington, VA 22217
Attn: Dr. N. Perrone
        Code 474
(Copy No. 78)

Commander
Mare Island Naval Shipyard
Vallejo, CA 94592
(Design Division)
(Copy No. 79)

Commander
Portsmouth Naval Shipyard
Portsmouth, NH 03801
(Copy No. 80)

Supervisor of Shipbuilding,
  Conversion and Repair
General Dynamics Corporation
Electric Boat Division
Groton, CT 06340
Attn: Dr. Robert M. Gorman
        Dept. 440
(Copy Nos. 81 and 82)

Supervisor of Shipbuilding,
  Conversion and Repair
Ingalls Shipbuilding Corporation
Pascagoula, MS 39567
(Copy No. 83)

Supervisor of Shipbuilding,
  Conversion and Repair
Newport News Shipbuilding and Drydock Company
Newport News, VA 23607
(Copy No. 84)

Naval Ship Research and
  Development Center
Underwater Explosion Research
  Division
Code 780
Portsmouth, VA 23709
(Copy No. 85)

Naval Underwater Systems Center
New London Laboratory
New London, CT 06320
Attn: Mr. G. F. Carey
(Copy No. 86)

Naval Underwater Systems Center
New London Laboratory
New London, CT 06320
Attn: Dr. R. S. Woollett
(Copy No. 87)

Naval Undersea Warfare Center
San Diego, CA 92152
Attn: Mr. G. Coleman
(Copy No. 88)

Dr. J. Barger
Bolt Beranek and Newman, Inc.
50 Moulton Street
Cambridge, MA 02138
(Copy No. 89)

Dr. D. I. G. Jones
Air Force Materials Laboratory
Wright-Patterson Air Force Base
Ohio 45433
(Copy No. 90)

Dr. M. C. Junger, President
Cambridge Acoustical Associates, Inc.
1033 Massachusetts Avenue
Cambridge, MA 02138
(Copy No. 91)

Acquisitions Supervisor
Technical Information Service
American Institute of Aeronautics
  and Astronautics, Inc.
750 Third Avenue
New York, NY 10017
(Copy No. 92)

Dr. R. S. Ayre
Department of Civil Engineering
University of Colorado
Boulder, CO 80302
(Copy No. 93)

Dr. D. Frederick
Chairman, Engineering Science and Mechanics
   Department
Virginia Polytechnic Institute and State
   University
Blacksburg, VA 24061
(Copy No. 94)

Dr. D. E. Hudson
Department of Mechanics
California Institute of Technology
Pasadena, CA 91109
(Copy No. 95)

Dr. G. Herrmann, Chairman
Department of Applied Mechanics
Stanford University
Stanford, CA 94305
(Copy No. 96)

Dr. A. Kalnins
Department of Mechanical Engineering
   and Mechanics
Leheigh University
Bethlehem, PA 18015
(Copy No. 97)

Dr. D. D. Kana
Southwest Research Institute
8500 Culebra Road
San Antonio, TX 78206
(Copy No. 98)

Dr. Y. -H. Pao, Chairman
Department of Theoretical and Applied
   Mechanics
Cornell University
Ithaca
New York, NY 14850
(Copy No. 99)

Dr. J. R. Rice
School of Engineering
Brown University
Providence, RI 02912
(Copy No. 100)

Dr. P. S. Symonds
School of Engineering
Brown University
Providence, RI 02912
(Copy No. 101)

Dr. W. J. Worley
Department of Theoretical and
   Applied Mechanics
University of Illinois
Urbana, IL 61801
(Copy No. 102)

Dr. Dana Young
Southwest Research Institute
8500 Culebra Road
San Antonio, TX 78206
(Copy No. 103)

Commander
Naval Sea Systems Command
Department of the Navy
Washington, DC 20362
Attn: SEA-09G32-Library
(Copy Nos. 104 and 105)